

Autonomous Telescopes: Wallace Observatory Impact and Preliminary Results

by

Molly Kosiarek

Submitted to the Department of Earth, Atmospheric and Planetary
Sciences

in partial fulfillment of the requirements for the degree of

Bachelor of Science in Earth, Atmospheric and Planetary Sciences

at the

MASSACHUSETTS INSTITUTE OF TECHNOLOGY

June 2015

© Massachusetts Institute of Technology 2015. All rights reserved.

Author
Department of Earth, Atmospheric and Planetary Sciences
May 18, 2015

Certified by
Richard Binzel
Professor
Thesis Supervisor

Certified by
Michael Person
Research Scientist
Thesis Supervisor

Accepted by
Richard Binzel
Chairman, Department Committee on Undergraduate Theses

Autonomous Telescopes: Wallace Observatory Impact and Preliminary Results

by

Molly Kosiarek

Submitted to the Department of Earth, Atmospheric and Planetary Sciences
on May 18, 2015, in partial fulfillment of the
requirements for the degree of
Bachelor of Science in Earth, Atmospheric and Planetary Sciences

Abstract

The construction and characterization of an autonomous telescope began in Fall 2014 at the MIT George R. Wallace, Jr. Astrophysical Observatory. An 11-inch Cassegrain Telescope was assembled in a 10-foot Technical Innovations ProDome. This telescope, the Small AUtonomous Robotic Optical Nightwatcher (SAURON), has the potential to autonomously collect photometric images. Data were taken on T-And0-15785, an eclipsing binary star, in order to test and characterize the system. The out-of-ecliptic R magnitude of T-And0-15785 was found to be 13.487 ± 0.016 . The magnitude changes for the primary and secondary eclipses were found to be 0.72 ± 0.036 and 0.62 ± 0.031 R magnitudes respectively. The telescope, SAURON, is currently able to locate targets and collect data robotically with an observer monitoring from afar.

Thesis Supervisor: Richard Binzel
Title: Professor

Thesis Supervisor: Michael Person
Title: Research Scientist

Acknowledgments

I would like to thank my advisor, Rick Binzel, for all of his advice regarding my thesis, classes, and academic career. I benefited from the mentoring of Michael Person throughout this whole process. I want to acknowledge Tim Brothers for his patient teaching at Wallace and for his vast knowledge of telescope operation. I could not have produced this thesis without Jane Connor for helping turn many unstructured thoughts into a readable thesis. I am very grateful for everyone who came to the observatory with me as I would not have been able to collect nearly as much data otherwise. I want to extend a special thank you to Jacobi Vaughn, my absolutely wonderful fiance, for all of the times that he came to the observatory, for proofreading my thesis, and for listening to me talk about nothing but telescopes for weeks. Lastly, I appreciate all of the advice and guidance that Rachel Bowens-Rubin has given me regarding astronomy, data, and life at MIT.

Contents

1	Introduction	13
1.1	Life at Wallace Astrophysical Observatory (WAO)	13
1.2	Motivation for Autonomous Telescopes	16
1.3	Valuable Research Projects	17
1.4	Application to WAO	18
1.5	Engineering Summary	18
1.6	Future Science Applications for WAO	19
1.7	Science Demonstration Target: T-And0-15785	19
2	Telescope Components and Construction	21
2.1	Components and Characterizations	21
2.1.1	Dome Components	21
2.1.2	Telescope and Mount Components	22
2.2	Instrumentation	22
2.3	Software	23
2.4	Construction	24
2.4.1	Dome and Telescope Construction	24
2.4.2	System Testing	27
2.5	Key Challenges	27
2.5.1	Dome Rotation	27
2.5.2	Sealing the Dome	29
2.5.3	Other Challenges	30

3 Science Implementation Demonstration	33
3.1 Data Collection	33
3.1.1 Observation Plan	33
3.2 Data Analysis	35
3.2.1 Data Reduction	35
3.3 T-and0-15785 Photometry Analysis	37
3.3.1 T-And0-15785 Results	43
3.4 Discussion	52
4 Conclusion	53
4.1 An Automated Dome and Telescope	53
4.2 Future Work	54
4.3 Long-Term Application	54
A Component Specifications	57
B Photographs	61
B.1 Photographs of Build Process	61
B.2 Reference Photographs for Construction	61
C Limiting Magnitude Calculation	71

List of Figures

3-1	Data Reduction Example	36
3-2	Fields for T-And0-15785	38
3-3	Relative Fluxes of Comparison Stars	42
3-4	Apparent R Magnitude of T-And0-15785	44
3-5	Folded T-And0-15785 Light Curve	45
3-6	Period Testing of T-And0-15785	51
B-1	Photos of Build Process	65
B-2	Dome Parts	69
C-1	Reduced Pleiades Image	72

List of Tables

3.1	Data Collection and Calibration	34
3.2	Data Reduction for T-and0-15785	35
3.3	Comparison Star Magnitudes	39
3.4	Comparison Stars for T-And0-15785	40
A.1	OTA Specifications	57
A.2	Mount Specifications	57
A.3	PICO Detector Specifications	58
A.4	QSI Detector Specifications	58
A.5	SBIG Detector Specifications	58
A.6	Software	59
C.1	Limiting Magnitude Calculation	73

Chapter 1

Introduction

1.1 Life at Wallace Astrophysical Observatory (WAO)

The Massachusetts Institute of Technology (MIT) George R. Wallace, Jr. Astrophysical Observatory (WAO) located in Westford, Massachusetts currently operates six permanent telescopes that are used by MIT graduate students, undergraduate students, and staff. These telescopes are typically used by novice students to learn basic telescope operation and by experienced students, staff, and faculty to observe occultations, measure exoplanet transits, and find asteroid light curves.

These six telescopes fall into three operational categories: manual, robotic, and remote. Manual telescopes require the observer to point the telescope at the target object. The observer first uses the finder scope to center a bright star in the field. Then they set the right ascension and declination wheels by using that bright star as a reference point; finally they are able to use these wheels to point the telescope at the target object. A robotic telescope connects to software that is able to point to the target object without the observer physically moving the telescope. However, the observer must still be at the same location as the telescope in order to fine-tune and troubleshoot the pointing. Remote telescopes can be operated from a different location by connecting to the computer which operates the telescope. An observer still needs to monitor the telescope while taking data; however, they do not need to

physically be co-located near the telescope. WAO has two 14-inch manual telescopes, two 14-inch robotic and remote telescopes, one 16-inch robotic telescope, and one 24-inch robotic telescope.

A typical observing night operates differently depending on the experience of the observer, the purpose of the project, and the weather for that night. A beginning student observer is typically taking the astronomy class 12.410J: Observational Techniques of Optical Astronomy. Their main goal is to learn how to operate a telescope and to successfully take a few hours of data over the course of the semester. They observe once a week for six to eight weeks, weather permitting.

An average night of observing for the student operates as follows: at 7:00pm the student gathers in a classroom on campus with the five other students in their lab section. Their teaching assistant or professor then drives them out to WAO. An hour later, 8:00pm, they arrive at the observatory and spend the first half-hour setting up the telescope. This setup includes turning on all of the instrumentation, cooling and focusing the camera, and determining their target location. If the student is on a robotic telescope, they are able to find their target object in as few as ten minutes. If the student is instead using a manual telescope, finding their target can take up to thirty minutes. By 9:00pm, the student begins to take data. After a few minutes of testing exposure times and determining the correct filter to use, the student will set the camera on a "continuous images" mode which takes a specified type data for a set time period. The student can then go inside and work on homework or study until 11:30pm. Throughout the continuous exposures, it is necessary for the student to check on their telescope every few minutes in case of error. At 11:30pm the student takes calibration images, transfers data to a server, and heads home. They arrive back on campus at 1:00am, having spent six hours to get two-and-a-half hours of data and two-and-a-half hours of interrupted studying. Overall, the observing knowledge that they have gained was worth the time spent and the requisite alteration of their sleep schedule. Their main mission was to learn how to operate a telescope, and once the

class finishes, they have succeeded.

However, the main goal for an experienced student observer, professor, or staff is to take data in order to use the data for research instead of the observational learning process. For them, a typical observing night is more streamlined. The night starts an hour before sunset, as the observer makes the hour long drive out to WAO. They first set up, cool and focus the camera, and locate their target in about thirty minutes. Afterwards, they start taking data. Assuming that the data-taking is going smoothly, the observer makes quick checks on the telescope every fifteen minutes, but can multitask otherwise. After some number of hours of observing, dependent on the weather and whether the observer has morning commitments the next day, the observer will take calibration data, transfer the data, and shut down. Most professors have daytime schedules and cannot afford to be night-shifted during the week. During the winter months, professors can typically observe from 5:00pm to 11:00pm, which results in three-and-a-half hours of data and an equivalent amount of time of interrupted work. During the summer observing occurs from 7:00pm to 11:00pm, which results in one-and-a-half hours of data. This commitment takes time away from families and extends their working day. This time sink is much less worth it for the experienced observer as they desire more data and therefore need more or longer nights of data. However, they are not gaining useful experience out of repeatedly setting up, watching, and shutting down the telescope. They would prefer to have full nights of data, sundown to sunrise, but can rarely commit that much time to data collection. They have daytime commitments which they must adhere to, families to go home to, and a sleep schedule to maintain.

What if the telescopes could operate themselves autonomously? WAO has been actively working towards this goal for two years now. This goal was first imagined by Professor Jim Elliot at WAO. Two of the six telescopes have remote capabilities; this capability allows experienced observers to operate them from campus. Operating the telescopes from campus saves the observer a few hours since they do not need to drive

to the observatory; however, they must still spend time setting up, operating, and shutting down the telescope. The next step would be to make a telescope autonomous. An autonomous telescope is able to operate throughout the night without the aid of a human. The autonomy would increase the efficiency of the telescope use without needlessly requiring observer time. The autonomous telescope would be able to take data every clear night, instead of being constrained by observer schedules. Telescope operation is similar to driving a car. A novice driver needs to be very attentive over the entire route and therefore has very little downtime. An experienced driver still needs to be constantly attentive, but can manage to uphold a conversation, listen to music, or otherwise think about something else. An autonomous telescope would be equivalent to riding in the backseat; you end up arriving at your destination without needing to do any work during the drive.

1.2 Motivation for Autonomous Telescopes

Small telescopes, less than a meter in size, are located at hundreds of universities for teaching and research purposes. These telescopes are meaningful resources which allow students to experience astronomy hands-on. However, as described above regarding WAO, the use of these telescopes can be very time-consuming even for an experienced observer. Between teaching, researching, and taking classes, students and professors do not have enough time to use the telescopes every clear night. As a result, many small telescope hours go unused at university observatories. Although university observatory's telescopes are small, they can collect useful data. Small, less than meter-sized, telescopes are especially useful for observation projects that need large amounts of observing time and modest precision [3].

Autonomous telescopes are an effective innovation to connect the availability of small telescopes with a long time series of repeated observations of a target object or field. Observers do not have enough time to use the university telescopes every opportunity; autonomous telescopes would be able to operate regardless of observer

availability. The autonomous telescopes would be able to take repeated observations of a target object or field with very little setup, since the data taking properties, such as field location, filter, and exposure time, would be consistent between nights. Many astronomy projects require repeated observations of the same object or field over the course of weeks or even months. Efficient use of existing telescopes can facilitate astronomy projects that require a lot of repeated viewing.

For example, the Transiting Exoplanet Satellite Survey (TESS) mission’s goal is to identify transiting exoplanets with host stars between fifth and twelfth magnitude [12]. Small telescopes will be needed to follow up on these exoplanet candidates to observe further transits and therefore confirm or deny the object as an exoplanet. These telescopes need to be smaller than one meter so that the bright host stars do not over saturate the Charge Coupled Device (CCD) and also will need to observe the transit for multiple orbital cycles (3-10 nights of observation) in order to make a confirmation. This sort of observing would be ideal for an autonomous telescope because of their accuracy and efficiency with little human input.

1.3 Valuable Research Projects

There are many projects similar to the TESS that can optimally be done with an autonomous small telescope. Determining the light curve of an asteroid, Kuiper Belt object, or eclipsing binary star would be a valuable project for an autonomous telescope since each of these projects require repeated observations. Astrometric measurements of an asteroid or Kuiper Belt object would also be ideal for an autonomous telescope since determining the position of an object requires many observations while the object moves in reference to background stars. If enough measurements of the position of an object in comparison to reference stars are obtained, the orbital solution of that object can also be determined. Projects, such as discovering asteroids or planetary satellites, that require a lot of telescope time can also be completed. Once an algorithm for searching the sky is written, the autonomous telescope can

follow the algorithm over successive nights and compare the images collected with a star database. Any deviations from the database can be investigated to see if the object moves similarly to a known asteroid or satellite. In short, small telescopes could contribute to a lot of projects if only they were easy and efficient to use full-time. Therefore, autonomous telescopes are an excellent tool for many observational projects.

1.4 Application to WAO

WAO and similar observatories have scientific potential that is not fully utilized. The telescopes could be used more efficiently and productively if they were operated every clear night. The telescopes would also be more cost-effective per datum if the amount of data collected per telescope increased. In order to increase the amount of data-taking potential at WAO, I began the construction and characterization of an autonomous telescope. This telescope, the Small AUtonomous Robotic Optical Nightwatcher (SAURON), will be able to observe throughout the night without the aid of a human. SAURON will allow the observer to sleep through the night and more efficiently use their time for research and classwork instead of monitoring and controlling the telescope. The autonomous nature of SAURON will allow it to be used whenever the sky is clear, whether or not an observer is available on site. This increased and more efficient use of telescope time will expand the data-taking potential of WAO and allow longer-term projects to be pursued.

1.5 Engineering Summary

I, with help from the Observatory Site Manager Tim Brothers, assembled SAURON, an 11-inch Celestron optical tube mounted on a Software Bisque Paramount ME II. SAURON is located in a 10-foot Technical Innovations ProDome at the Massachusetts Institute of Technology George R. Wallace, Jr. Astrophysical Observatory. We constructed the dome and assembled telescope components during Summer 2014. We

then tested the overall setup and troubleshooted initial problems over Fall 2014. From January through March 2015 operational testing was performed by collecting eclipsing binary star data while I considered how to make the dome more cold and snow tolerant. The telescope is currently able to operate with a remote observer; however, weather and time constraints have yet to allow achievement of full autonomy. There are plans to complete the automation during Summer 2015.

1.6 Future Science Applications for WAO

Once this telescope is fully autonomously functioning, WAO will be able to collect science data more efficiently and use all possible clear nights regardless of the availability of observers. Also, two of WAO’s existing telescopes, the two 14-inch robotic telescopes, may be upgraded to be autonomous, which will further increase the efficiency of data collection.

This project has even larger implications for an observatory located in a non-ideal location, such as WAO which is located in an area with abundant cloudy nights, humid summers, and light pollution from surrounding cities. Because an autonomous telescope does not need human interaction, the physical telescope can be built far away from the location of the observers. The telescope can instead be located in a remote location which has optimal weather conditions. Therefore, this project allows the next WAO telescope to be built in a remote location, far away from the cloudy skies of the Northeastern United States.

1.7 Science Demonstration Target: T-And0-15785

In order to characterize the new telescope and troubleshoot during the building process, I gathered data on an eclipsing binary star, T-And0-15785. I chose this star because its baseline R magnitude of 13.830 is bright enough to view with a 10” telescope even in moderate weather conditions. The R magnitude change between the

baseline and eclipse is 0.703, which is also visible from the 10" telescope in favorable weather conditions. The period of the eclipsing binary star is 0.7311466 days, a short enough time period that I can gather a meaningful amount of the eclipse in one night. T-And0-15785 is located in the constellation of Andromeda at a right ascension of 01 03 13.82 RA and a declination of +47 59 46.6 which means that it was above the horizon over my data taking period, from January through March 2015 [2]. The full scientific demonstration is discussed in Chapter 3.

Chapter 2

Telescope Components and Construction

2.1 Components and Characterizations

2.1.1 Dome Components

The dome used for this project is a Technical Innovations 10 foot ProDome. In order to be autonomous, the telescope must be housed in a dome that can withstand and operate during all four seasons, can take conditional commands from the weather monitoring systems, and location commands from The SkyX via ASCOM. We chose the Technical Innovations Pro Dome in order to fit these requirements. The dome is mounted 24 inches above the ground on top of two support rings. This height was chosen so that the telescope mounted inside matches the shutter height and therefore can see the skies in all directions. The minimum observable altitude with this dome, given the current tree-line, is 40 degrees in the North, 10-15 degrees in the South, and varies around 20 degrees in the East and West. The majority of WAO's observations are concentrated in the South, as WAO focuses on solar system bodies, which are viewed in the southern area of the sky.

2.1.2 Telescope and Mount Components

The Optics system is a repurposed 11-inch Celestron NexStar GPS optical tube, mounted with a dovetail to the SoftwareBisque Paramount ME II. This optical tube was chosen since the Celestron NexStar telescope was currently unused at WAO and had the ability to be repurposed in order to test the autonomous abilities of the rest of the necessary components. This optical tube is not meant to be the final optical tube. Once the system is fully autonomous, there are plans to upgrade the optics to an 17-inch tube so that fainter targets can be observed. The mount brand was chosen because WAO has experience installing and running SoftwareBisque Paramounts. This mount specifically was chosen since it is capable of robotically pointing to target locations and has instrument capacity for 109 kg [9], which is compatible with both the preliminary 11-inch telescope and the final 17-inch telescope.

The Paramount is mounted on a custom-made steel pier designed by Brothers and fabricated by the MIT Haystack Observatory. The pier is located nearly in the center of the dome and is bolted to a 18" wide, 39.5" tall, concrete cylinder with a steel pipe that was previously built at WAO. This concrete pier is resting on underlying bedrock and stabilized by the surrounding concrete so that surface vibrations caused by dome movement, human interaction, or wildlife do not affect the telescope. More information about the Optics and Mount Specifications can be found in Appendix A.

2.2 Instrumentation

Over the course of this project, three different Charge-Coupled Devices (CCD) were used: Portable Instrument for Capturing Occultations (PICO) [4], Quantum Scientific Imaging (QSI) 683s CCD, and Santa Barbara Instrument Group (SBIG) ST7-XME Detector. Each of these cameras are temporary cameras; a new camera will be purchased for this project when the entire system is fully autonomous.

Brothers and Dr. Michael Person, Director of WAO, initially chose the PICO

camera since it has a 12x12 arcminute field of view, directly connects to the filter wheel, and there was one available at WAO [4]. The PICO camera was used until mid-January when the shutter was not reliably opening due to the extreme cold. The QSI 68s CCD is typically used on one of the telescopes used for classes at WAO. Since normal classes were not in session over January, I was able to use the QSI camera. The QSI camera has a field of view of 20 arcmin 57 arcsec x 15 arcmin 46 arcsec [10] which made it easier to find the target object and therefore aided troubleshooting. Once classes required the QSI camera again, I made the last switch to the SBIG ST7-XME. This camera had the smallest field of view at 8 arcmin 2 arcsec x 5 arcmin 21 arcsec [8] and was therefore the least ideal since very few comparison stars could be located in image frames.

Other necessary instruments include: Starlight Xpress USB filter wheel, Custom Scientific Johnson/Cousins Photometric BVRIC filters, and Integrated-Control Temperature Compensating Focuser (TCF-Si). The filter wheel is a 5 position, 2" plate and has T adapters on both sides. Other necessary components include: computer, monitor, keyboard, mouse, security camera, programmable power outlets, UPC, fan, and industrial USB hub.

2.3 Software

A wide variety of software was used at different steps in the automation process. General programs required for operation include: MasterSync and Sophos Endpoint Security and Control. Programs required for dome and telescope control include: The SkyX Pro, Tpoint Add On, Optec TCF-S 64, CCD drivers, and Digital Dome Works. Programs that will be required for automation include: CCDWare's CCDAutoPilot. Other programs used include: Chrome, Secure FX, AstroImageJ, MaximDL. A full list of programs and their uses is located in Table A.6 in Appendix A.

2.4 Construction

2.4.1 Dome and Telescope Construction

The construction of this imaging system had several distinct steps: setting up the surroundings, constructing the dome, setting up the other components and finally testing the system. Originally, the north-west side of WAO only contained a four-foot concrete pier in the center of a concrete pad. First, unused telephone poles near the pad were taken down on 5 May 2014. A trench was dug around the perimeter of the pad and filled with crushed stone for drainage on 13 May. A Cat5E cable, a 1x20A 110V circuit, and two ethernet cables were run from the pad to the main building through PVC pipe. All of the electrical work was done by Lee Pothier, Jon Byford and Brothers. Next, ten oak trees were taken down on the north side of the site so that Polaris can be seen from the pad to polar align the telescope and so that the minimum altitude observable in the north is lower. Excavation work was done by Legace of Westford, MA.

The original plan was to attach the paramount directly to the concrete pier; however, the concrete pier had cracks in several locations that penetrated all the way to the steel pipe in the center of the pier and cracks that went down nearly to the pad height due to weathering for nearly thirty years. Neither the pier nor the steel pipe were plumb. After qualitative analysis by Chris Eckert, we agreed that the structural integrity of the pier had been compromised. Our solution was to demolish the existing pier to the point where no cracks continue, which is just above 6" from the concrete pad. A 30" Permanent steel Pier was purchased from SoftwareBisque to increase the height of the pier. The paramount is attached directly to this permanent steel pier. This height allows the optical tube to be as low as possible due to zenith issues, but high enough to see over the 36" dome base.

The dome was constructed from 16 July to 11 August. A picture summary is located in Appendix B. It arrived on 16 July and was delivered to a nearby MIT

observatory, Haystack Observatory, where we unloaded the crate with a forklift and brought the individual pieces over to WAO by truck. The crate was no longer structural once it was removed from the truck. Once the pieces were at WAO, we sorted them and laid them out in the grass in the approximate configuration for construction. Each of the three dome rings, one base ring and two support rings, were separated into six separate pieces. We first placed these pieces onto the concrete pad and loosely bolted them together. Using a string and a level, we measured the circumference at different positions in order to circularize the dome. After the dome was approximately circular, we tightly bolted the pieces together and continued measuring. In the end, the dome is 119.5 inches in diameter and less than or equal to 0.3 degrees off of level. Once the dome ring was sufficiently circular, we drilled half-inch holes into the concrete and attached the ring to the pad with 20 lag screws and lag shield anchors.

Next, we bolted the dome roof halves together on 18 July. The dome roof did not have counter-sunk holes for the bolts to fit into. Instead, when the bolts were fully tightened, they created a permanent indent into the fiberglass dome material. Then we attached the two pieces of the dome roof to the dome support ring with the three shutter pieces in-between them. Brothers machined and installed a metal bar vertically from the concrete pad to the dome wall next to the open-side of the door in order to keep that section from bowing out when not attached to the door. On 18 September we completed the dome wiring. I then used cable ties to attach all of the cables onto the dome walls so that they would be grouped together and off of the floor. Next I assembled an ethernet cable to connect the dome to the main building. As a result of all of the cabling, the dome now had rotational capabilities.

In order to automate the shutter, cables needed to be strung along the edge of the shutter, attached to the motor in the back, and made taught with shutter clamps. These shutter clamps were missing from the original shipment. After communicating with Technical Innovations for over 3 weeks and miscommunicating about shipping

locations, we received an incomplete set of two different types of shutter clamps. I therefore machined three shutter clamps myself on 18 September to complete one set of shutter clamps. Afterwards, we threaded the cable through the tracks on the shutter and tightened the cables. Gloves are a necessity when working with metal cables.

Preliminary testing of the dome was done with the hand paddle that is wired directly to the control board in the dome and with the homing switch on the outside of the dome. The dome successfully rotated in both directions, found locations around the dome, found the home position, and opened the shutter. However, the shutter did not close. After examining the hand paddle and control board for errors we found part of the control panel was defective. Brothers determined that we needed to send the control board back. Brothers and I ended up reversing the wires on the motor and using the open key on the outside of the dome to close the dome.

Once the dome was operational and fully sealed off from the weather, I began to move the telescope components outside. First, I bolted the Paramount ME II to the SoftwareBisque steel pier and leveled the mount using the microlevelers at the base of the mount. The mount is level within 0.1 degrees, the uncertainty of the level. On 25 September I moved all of the other instrumentation, telescope, camera, focuser, computer, filter wheel, UPC, security camera, and remote controlled power strip outside to the dome. Before attaching the OTA to the mount, I threaded all of the necessary cables through the mount so that none of the cords can get wrapped around the mount during operation. Preliminary daytime testing showed that everything was in working order. The SkyX - the program that controls the mount, camera, focuser, and filter wheel - was also able to connect to the dome.

2.4.2 System Testing

A number of calibrations were done in order to have an operational telescope, including: polar alignment, mount Periodic Error Correction, and Tpoint mapping. I operated the telescope at night for the first time on 2 October. That night I first tried to drift-polar-align the telescope. Steps for the drift-polar-alignment were found in the Sky and Telescope magazine [5]. The park position for the telescope was then set at horizontal pointing west. This position was chosen so that the dome can be accessed during the day without having the telescope point at the sun.

After the mount was polar aligned, I determined the Periodic Error Correction (PEC) with The SkyX in order to track targets over long periods of time. Periodic error is the mechanical error induced by the mount as the gears complete full revolutions. The error is periodic over those revolutions, and can therefore be calibrated out to produce more exact tracking. The next calibration that was completed was Tpoint mapping. The SkyX has a Tpoint add-on that traverses the sky and compares the position of the mount and intended location on the sky with the actual location on the sky. To find the actual location The SkyX uses an astrometry routine to compare the image field with a variety of star catalogs and determine the pointing error. Tpoint can then be used to create a model for the mount that adapts the speed and direction of the motors as they are moving in order to more accurately reach a target location.

2.5 Key Challenges

2.5.1 Dome Rotation

While data were being taken in January, the dome began to have rotation errors. When the dome first stuck in one location, around 100 degrees, The SkyX continued to send dome commands without timing out. The dome status switched between "Ready" and "Slewing to target" continuously since The SkyX was programmed to

keep the dome in line with the telescope. Since the software was still actively trying to move the dome, it would not accept any more commands and therefore I disconnected the dome from The SkyX. I opened up Digital Dome Works (DDW) and tried to rotate the dome through 100 degrees in the clockwise direction, as The SkyX was trying to do, with no success. DDW does time-out after a few seconds of no movement, allowing more commands to be entered. I was able to rotate the dome counterclockwise through 100 degrees. Once the dome was past the problem area, it was able to continue tracking the telescope.

As January progressed, the dome got stuck at more locations, including 100, 110, 220, and 290 degrees, culminating on 2 March where I was unable to automatically close the shutter. I was able to manually push the dome through the problem areas, reach the home position, and therefore close the shutter. The dome software first checks to make sure that the dome is home before initiating the "shutter close" command. In the case of error, however, it would be optimal to be able to close the shutter even when the dome is not homed, especially when it is not possible to reach the dome location and manually push the dome. However, the shutter motors are not connected to power when the dome is not in the home position; therefore, the dome design would need to be altered in order for this change to be possible.

During the day, Brothers, Person, and I evaluated the dome rotation and found problems from ice warping the dome to collisions between the dome support ring (DSR) door hinge screws with the dome wall. When the dome is pointing towards 110 degrees, the DSR buckles upwards so that there is minimal contact between the dome and support wheels in that area. There are two motors, one on the east side and one on the west side. This buckling causes one of the DSR door hinge screws to make contact with the side of the dome wall which prevents rotation. After redrilling some holes to make the screws flush with the side, the 110 degree section no longer completely stopped the movement. We then found that the buckling also causes the East motor to not come into contact with the dome track, and the West motor is

then overwhelmed. After further investigation of the support wheels, we found that between one-third and one-half of the wheels typically do not contact the dome support ring. After calling Technical Innovations and receiving no response, we decided to halve the length of the spring on the east motor in order to provide more contact between the motor and the dome track. Pending further evaluation, we may try shimming the DSR area in order to decrease the amount of buckling.

Around March, we realized that the cold amplifies the dome traction problems. Most directly, we determined that ice had entered one of the dome seams and caused a small amount of warping. Many of the dome ring and DSR screws needed to be tightened, since they were loosened from the warping. We countersunk more support wheel screws into the dome. Brothers replaced the West drive unit when it broke around 9 March. Throughout all of these problems, the drive belt had also been getting worse. By 13 March the dome rarely stuck during the day, while the weather was above freezing; however, it continued to stick frequently at night, while below freezing. The rubber wheels likely harden in the cold, and there could be some condensation on the track that turns to frost and results in less traction. Throughout all of this sticking, the motors have continued to turn and have ground off much of the traction material on the dome ring. There is now no traction material left at a couple of locations around the dome. I plan on applying a tacky friction paint to the entire dome ring once the weather improves.

2.5.2 Sealing the Dome

In order to seal the dome, caulk was applied both between each of the sections while construction was taking places and also applied externally in all crevices after construction was completed. Sealing off the dome from the weather is extremely important so that rainwater cannot get inside and harm the telescope or computer components and so that water cannot freeze between pieces, expand, and alter the shape of the dome. In order to produce a good seal, Megan Russel, Olivia Brode-

Rogers, Rachel Aviles, and I first loosened all of the pieces that came bolted together, caulked between the pieces, and quickly retightened each bolt. We also caulked between pieces as we bolted them together. Once the dome was constructed we also caulked around all exterior connections between pieces. Caulk itself was not sufficient to seal between the dome base and the concrete pad since the caulk would not adhere to the concrete. After applying caulk three times without successfully keeping water from seeping into the dome, Brothers used foundation sealer to seal this area.

Sealing the area beneath the door was difficult. We could not use the foundation sealer between the door and the concrete since that would prevent the door from being functional; the door requires a few centimeters of clearance from the ground to swing open. Our solution was to apply a 2-inch high barrier of foundation sealer on the inside of the door, so that water that runs underneath the door will be stopped by this barrier. However, this solution was not sufficient during large snowfalls. During February, snow piled up against the caulk next to the door. Water that melted from this snow pile was able to flow over the caulk near the door. This caulk successfully prevented rain from entering the dome; however with sufficient snow, the water built up and flowed over the caulk. My solution was to keep all electronics away from the door. A longer term solution will be to increase the height of the foundation sealer, and possibly to add a small wall that can be stepped over instead of just foundation sealer.

2.5.3 Other Challenges

Homing Pad Area: The "home area" that is used by the telescope to determine whether it is located at the home position is three inches long. This size results in a difference in pointing by a few degrees depending on whether the dome reached the home area from the clockwise or counterclockwise direction. Although this difference makes no noticeable difference if the dome is only being used autonomously, this difference does affect the ability of the door to open. The dome needs to be

precisely homed in order for the door to open without contacting the dome ring. My solution has been to always close the dome from the same direction so that the dome is precisely home.

The SkyX Star Determination: Many SkyX functions, such as image link and autofocus, requires the SkyX to be able to determine which areas on the field are stars. When the CCD is not flat, the resulting bright spots can be located and assumed to be stars. The flatness of the PICO camera caused problems when I was Tpoint mapping; Image Link was unable to identify the field due to the bright areas of the CCD. Without Image Link working, an autonomous telescope cannot confirm that the telescope is pointing in the correct location. My solution was to take longer exposure images so that the brighter areas of the CCD were considerably dimmer than the field stars. For autofocus, The SkyX identifies one bright star in the field, repeatedly takes images of that spot, and tries to minimize the full-width half-max. When autofocus chooses a bright spot of the CCD instead of a star, the autofocus is very inaccurate. My solution was to manually focus while using the PICO camera; this solution is not sustainable when this telescope is autonomous.

PICO Shutter Issues: Due to the cold amplifying a mechanical issue with the PICO camera, the shutter frequently stuck in a partially-opened or fully-closed state and was therefore unable to take images. Initially, the problem could be solved by taking repeated one-second images to exercise the shutter. However, as the nights got colder, this method did not always work. I then had to turn off and disconnect the camera, physically go out to the dome and take the camera off of the telescope, manually exercise the shutter with a cotton swab, and reconnect the camera. My initial solution was to repeatedly take images throughout the night, even while slewing, so the shutter stayed in motion. My ultimate solution was to switch cameras to one that did not have this shutter problem.

Filter Wheel Startup: The filter wheel does not always check which filter it is on

when starting up. Therefore, The SkyX does not always initially display the correct filter. The solution is to always move the filter before taking the first image, since the filter does check placement when moving.

Powering On the Computer: We have not yet found a way to remotely power on a computer. I have been investigating a "Wake on Lan" approach, but have not yet gotten it to work. My current solution has been to keep the computer turned on, and manually press the power button to turn the computer on when it is accidentally turned off. This solution is not adequate for an autonomous telescope. A "Wake on Lan" or other wireless solution will be needed for an autonomous telescope.

Chapter 3

Science Implementation Demonstration

3.1 Data Collection

3.1.1 Observation Plan

To demonstrate the scientific capabilities of SAURON, eight nights of data were collected on T-And0-15785, an eclipsing binary star, from January through March 2014. I chose T-and0-15785 due to its availability during each night from January to March, low magnitude, large delta magnitude and short period. T-And0-15785 is located at 01 03 13.82 RA and +47 59 46.6 DEC in the constellation Andromeda. According to J. Devor et. al. 2008 [2], it has an R magnitude of 13.380 and varies by 0.703 over a period of 0.7311466 days. A summary of all observations can be found in Table 3.1.

Table 3.1: Data Collection and Calibration

Date	Conditions	Camera	Target	Filter	Operational Notes
1/07/15	clear, full moon	PICO	NGC 129, T-And0-15785	Clear	dome errors
1/10/15	clear, partial moon	PICO	T-And0-15785	Red	shutter issues
1/19/15	clear (until 12:00am) to cloudy.	PICO	T-And0-15785	Clear	shutter issues
1/20/15	patchy clouds to clear	PICO	T-and0-15785	Clear	dome has ice in it
1/22/15	clear, crescent moon.	PICO	T-and0-15785	Clear	full eclipse observed
1/23/15	clear (until 9:00pm) to cloudy	PICO	T-and0-15785	Clear	choppy flat curve
2/03/15	clear, full moon	QSI	T-and0-15785	Red	dome issues
3/06/15	clear to cloudy	SBIG-ST7	Pleiades	Clear	flats taken with BVRC filters
3/19/15	clear	SBIG-ST7	T-and0-15785	Clear	

3.2 Data Analysis

3.2.1 Data Reduction

All data were reduced and analyzed using AstroImageJ and Matlab. To reduce the data, I first collected bias frames, dark frames, and flat frames each night, when possible. The bias frames were collected using a zero second exposure time with the shutter closed. Bias frames are collected to examine the performance of the CCD with no incident light. Dark frames were collected with an exposure time equal to that of my data, which was typically 60 seconds and the shutter closed. Dark frames are taken to analyze how thermal current builds up over time on the CCD. Dark and bias frames are then subtracted from the data to calibrate out the read and thermal noise. The flats were taken at dusk with an exposure time needed to receive about 20,000 counts and the same filter as the data.

Table 3.2: Data Reduction for T-and0-15785

Local Date	# Images	Notes
01/07/2015	40	shutter problems, no flats
01/10/2015	20	shutter problems, no flats
01/19/2015	573	no flats
01/20/2015	93	no flats
01/22/2015	1117	no flats
01/23/2015	653	spotty data, clouds and shutter issues, no flats
02/03/2015	157	BVRC flats
03/19/2015	51	BVRC flats

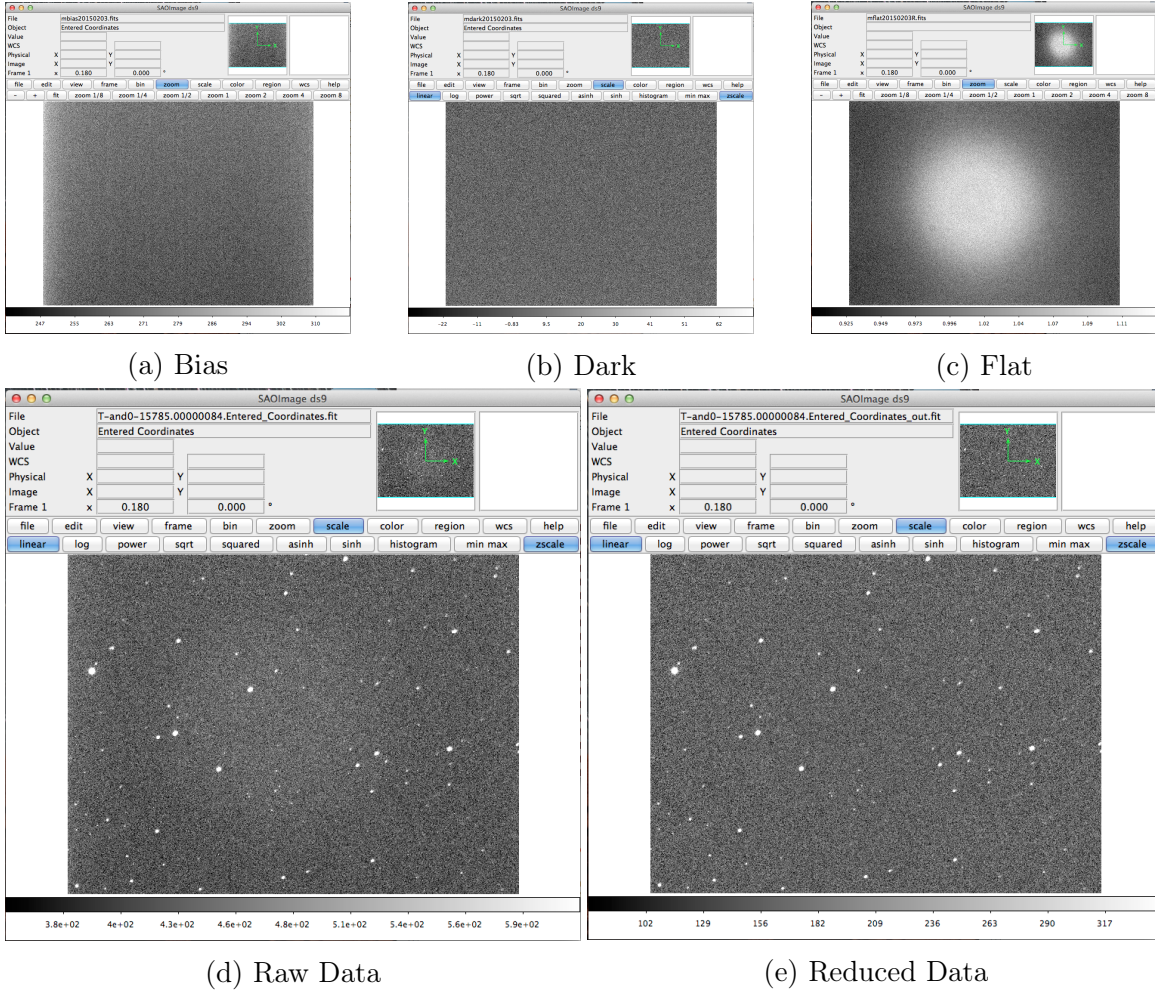
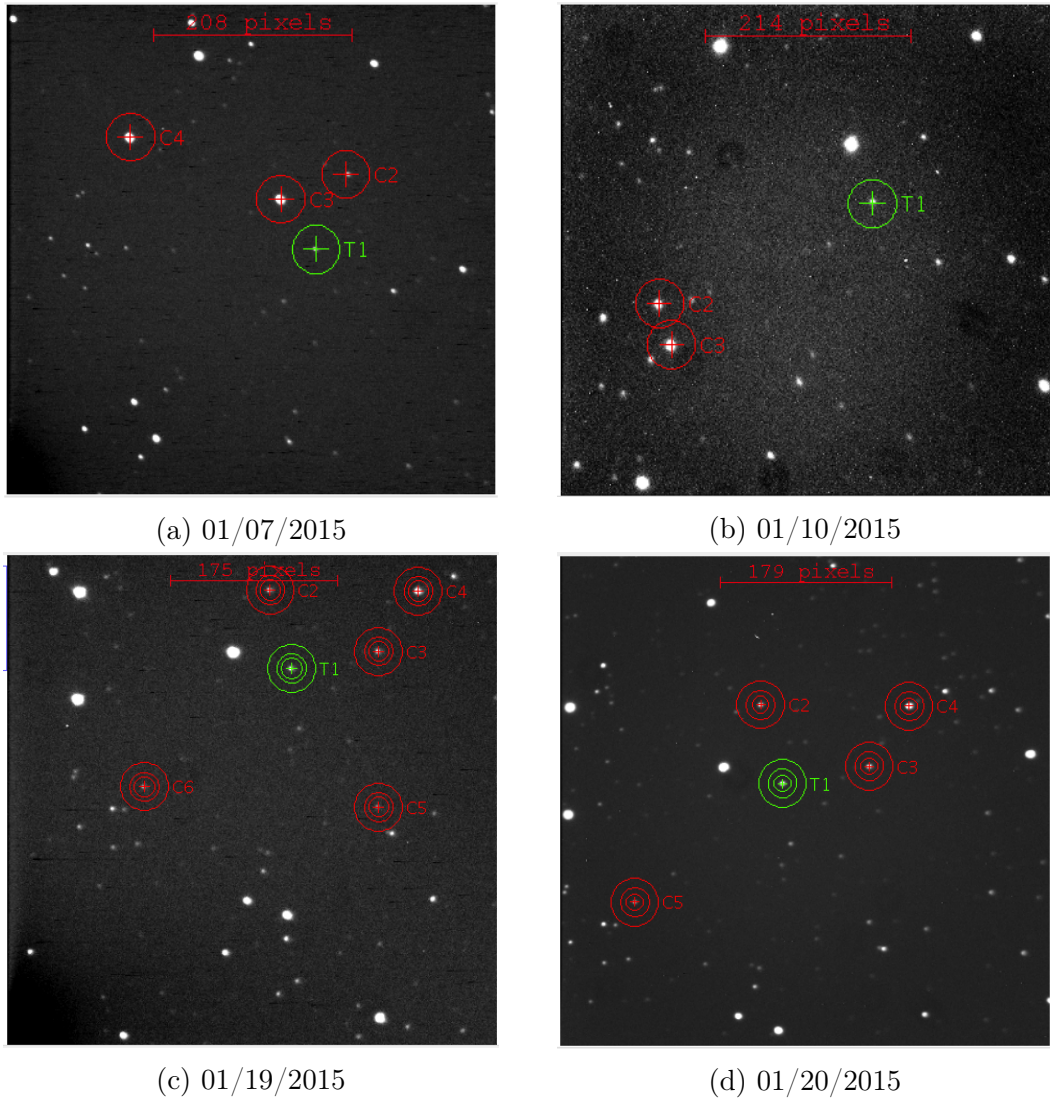


Figure 3-1: Data Reduction Example. An example calibration image of each type, bias, dark, and flat, is shown above. The raw data were taken on 3 February 2015 with an QSI camera in the R filter. The reduced data were reduced using AstroImageJ.

An example of my data reduction process is shown in Figure 3.1 above. All of the images were taken on February 3rd with the QSI camera. The first picture is a bias frame with an exposure time of zero seconds. The second is a dark frame with an exposure time of 60 seconds. The third is a flat frame with an exposure time of five seconds taken with the Red filter. The fourth image is the field of T-And0-18575 taken with an exposure time of 60 seconds and the Red filter. The fifth image is the reduced version of the forth image.

3.3 T-and0-15785 Photometry Analysis

I used a different set of comparison stars for data analysis each night due to a combination of different sky conditions, exposure times, cameras used, and field sizes. The field for each of my data taking night, along with all of the comparison stars used for data analysis, are shown below in Figure 3.2.



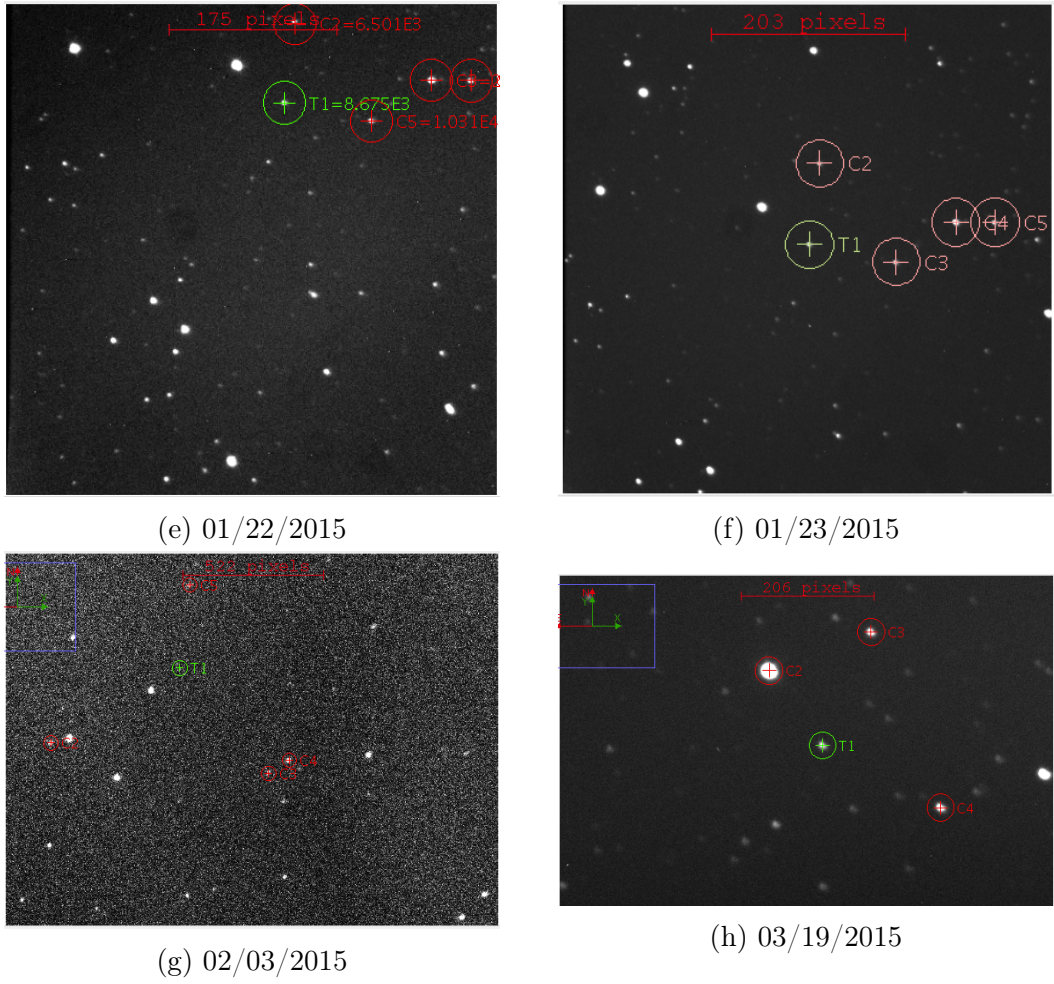


Figure 3-2: Fields for T-And0-15785. The field used for photometry analysis each day is shown with each comparison star and target star. The target star is labeled T1 and each comparison star is labeled C#.

In order to convert my plots from flux to magnitude, I performed differential photometry on my target star by comparing the flux from the target with the flux from the comparison stars. Using the comparison star's apparent magnitudes, I then converted the relative flux of my target star to apparent magnitude. Below are two tables. The first, Table 3.3, lists the right ascension (RA), declination (DEC), and R-magnitude of each star A through K. Each comparison star magnitude was found using the USNO-A2.0 Catalogue [7]. The assigned letter can be used in conjunction with Table 3.4 to associate each comparison star shown in Figure 3.3 with its specifications listed here. The second, Table 3.4, pairs each comparison star from the fields above with a star named A through K. The C# refers to the number of each comparison star shown in Figure 3.2. The suitable comparison stars determined in Figure 3.3 are also noted here. Only suitable comparison stars were used for analysis.

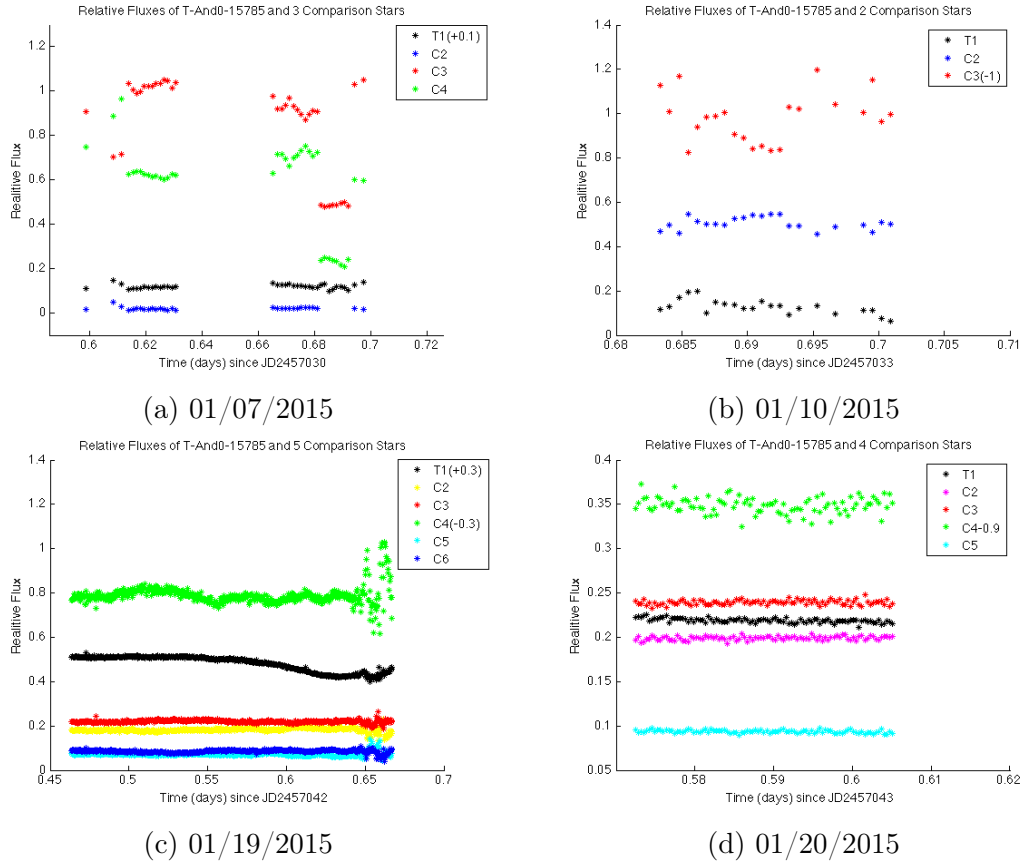
Table 3.3: Comparison Star Magnitudes

Assigned Letter	RA	DEC	Rmag
A	01 03 08.323	+47 58 01.01	13.9
B	01 02 52.710	+48 00 30.40	12.4
C	01 02 47.433	+48 00 49.49	13.6
D	01 03 02.961	+48 00 55.29	13.7
E	01 03 18.337	+48 03 39.98	14.7
F	01 03 41.308	+47 59 25.01	15.6
G	01 03 29.453	+47 54 05.23	11.4
H	01 03 41.675	+48 03 09.92	12.2
I	01 03 38.859	+48 04 05.56	11.7
J	01 03 18.441	+47 58 30.23	11.7
K	01 03 39.643	+47 56 45.60	11.1

Table 3.4: Comparison Stars for T-And0-15785

Date	C#	Assigned Letter	Suitable for analysis?
20150107	C2	A	Yes
	C3	J	Yes
	C4	K	Yes
20150110	C2	H	Yes
	C3	I	Yes
20150119	C2	A	Yes
	C3	D	Yes
	C4	B	Yes
	C5	E	No
	C6	F	No
20150120	C2	A	Yes
	C3	D	Yes
	C4	B	Yes
	C5	F	No
20150122	C2	A	Yes
	C3	B	No
	C4	C	Yes
	C5	D	Yes
20150123	C2	A	Yes
	C3	D	Yes
	C4	B	Yes
	C5	C	Yes
	C2	G	No
20150203	C3	H	Yes
	C4	I	Yes
	C5	B	Yes
20150319	C2	J	No
	C3	A	Yes
	C4	D	Yes

First, I determined if all of my comparison stars were suitable for use. In order to be suitable, the comparison star needs to have a constant flux relative to the other comparison stars and also needs to have a large enough signal-to-noise ratio. Below, in Figure 3.3, are the plots for each comparison star's flux relative to each other comparison star. The target star is also shown in these plots relative to all comparison stars; in most cases, the target star does not have a constant relative flux amount since the binary stars are eclipsing.



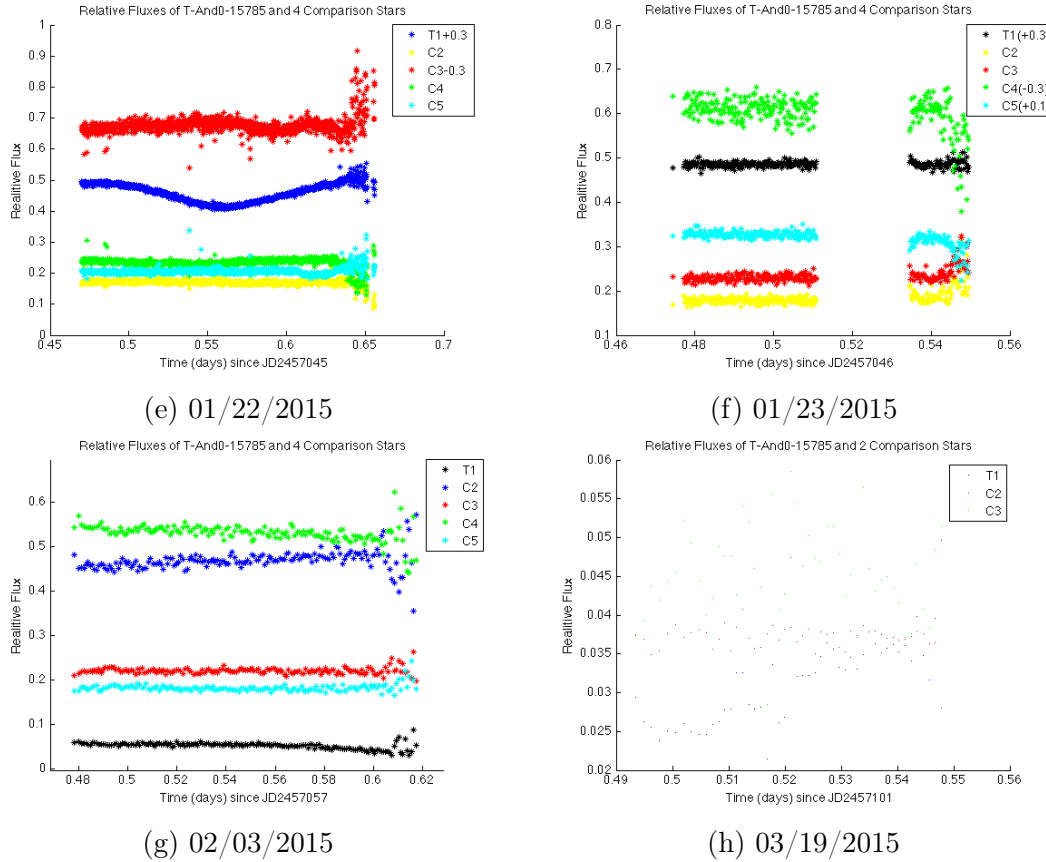


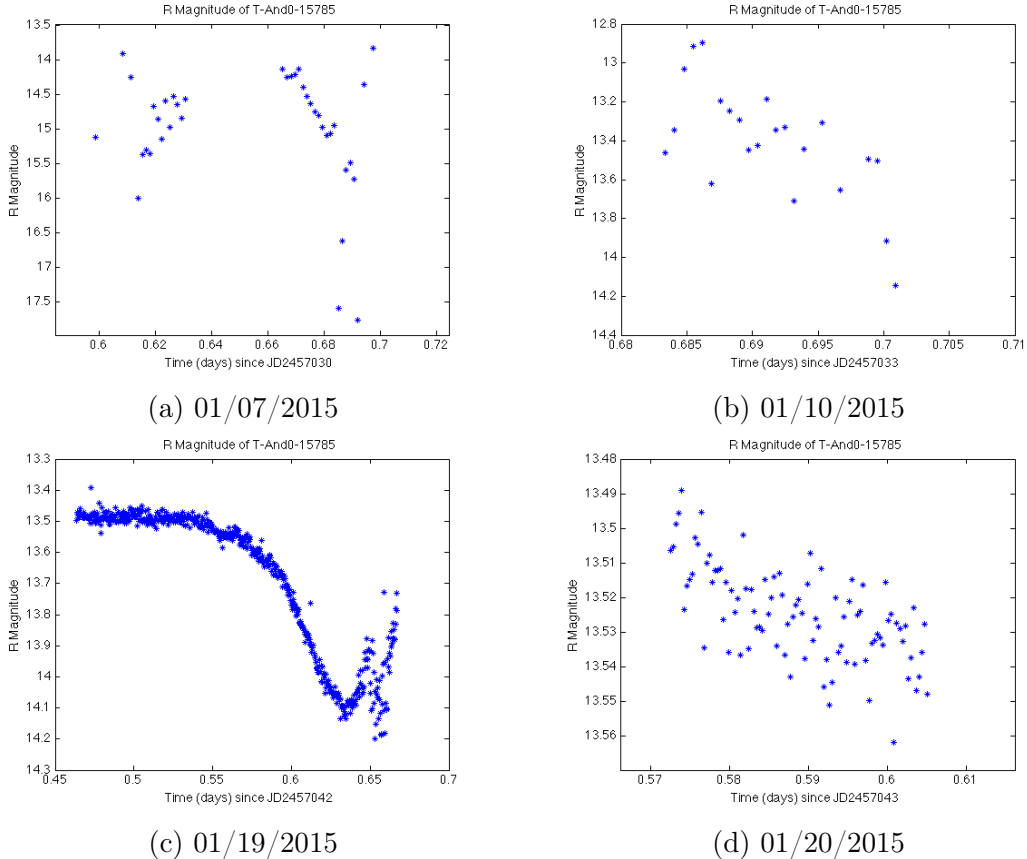
Figure 3-3: Relative Fluxes of Comparison Stars. The target star is listed as T1 and comparison stars are listed as C#. Some of the fluxes were shifted on the graph in order for the fluxes to separate each flux vertically so that they could all be clearly seen. The amount that each flux was shifted is noted in the graph legend.

3.3.1 T-And0-15785 Results

I calculated the apparent R magnitude of T-And0-15785 over eight nights. Below, in Figure 3.4, are the apparent magnitude plots for T-And0-15785 for each observation night. These plots were created by comparing the flux counts for T-And0-15785 with the flux counts for the comparison stars listed in Table 3.3 and Table 3.4 and then converting the flux to magnitude using Equation 3.1 below.

$$m_T - m_0 = -2.5 \log_{10} \left(\frac{F_T}{F_0} \right) \quad (3.1)$$

Where m_T is the apparent magnitude of the target object, m_0 is the magnitude of a reference star, F_T is the flux from the target star and F_0 is the flux from the same reference star [11]. All fluxes should be observed in the same filter and will result in an apparent magnitude of that filter.



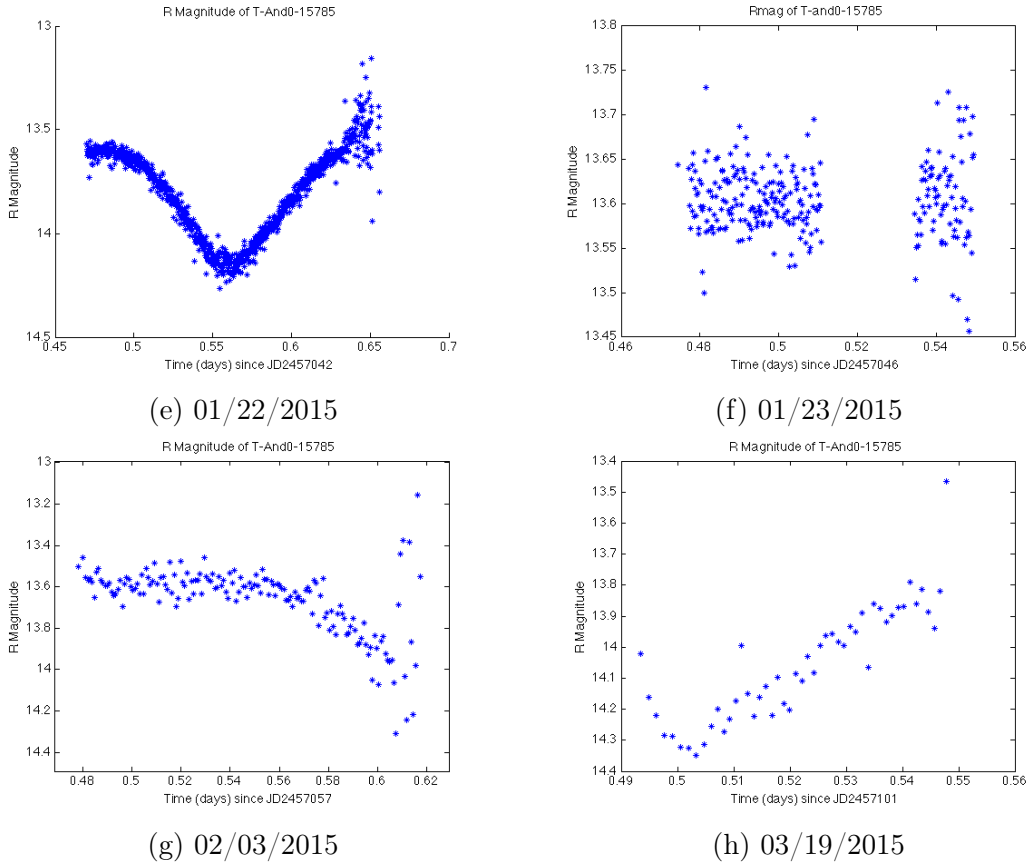


Figure 3-4: Apparent R Magnitude of T-And0-15785. Each plot shows the apparent R magnitude of T-And0-15785 for one data collection night. The magnitude was found by comparing the flux counts for T-And0-15785 with the flux counts for the comparison stars listed in Table 3.3 and Table 3.4 and then converting the flux to magnitude using Equation 3.1.

I folded this data over the period of 0.7311466 [2] to get the eclipsing binary star's light curve. I did not include 7 January or 10 January in the plot since neither of these days had reliable data. Both of these nights had lots of error from cloud cover and repeated breaks in the data collection in order to troubleshoot camera shutter issues and dome movement issues. This folding resulted in Figure 3.5 that includes both peaks of the eclipsing binary star system. The baseline was found to be 13.487 ± 0.016 by finding the average value of the baseline section of data points from 19 January 2015. This day was used because it had the longest baseline with the smallest standard deviation of error. The other three curves that included parts of the baseline were shifted to fit that baseline. 23 January was shifted 0.117 magnitudes down, 20 January was shifted 0.037 magnitudes down, 2 February was shifted 0.094 magnitudes down. 22 January and 19 March were unable to be shifted since they did not include any part of the baseline in the data.

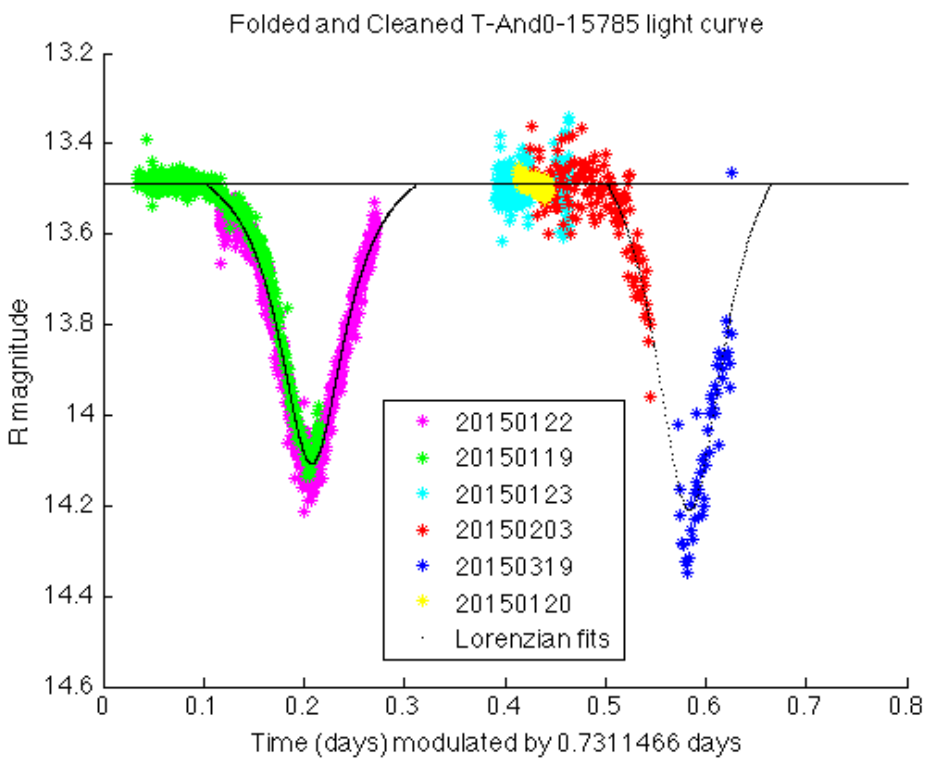
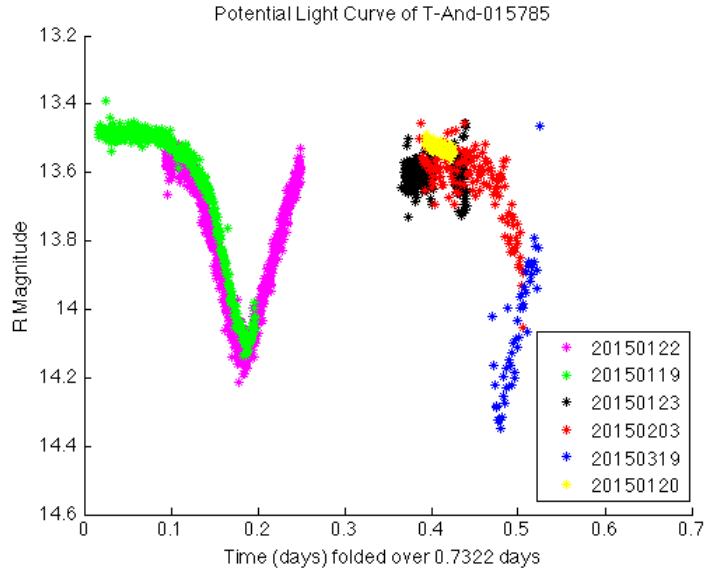
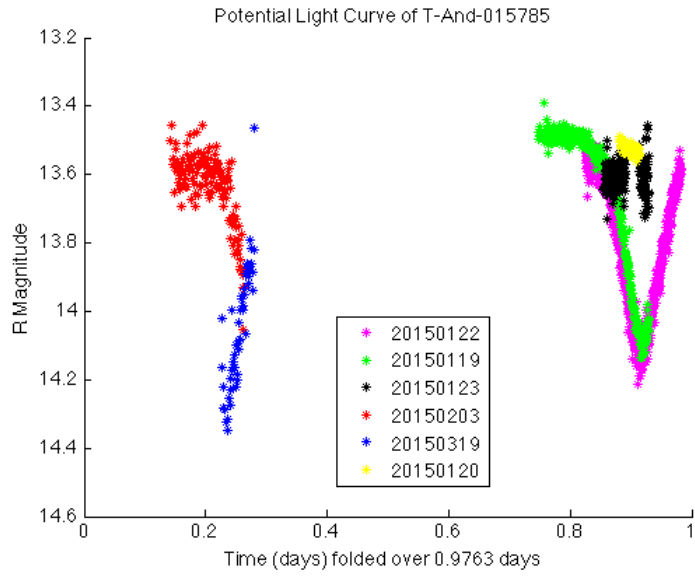
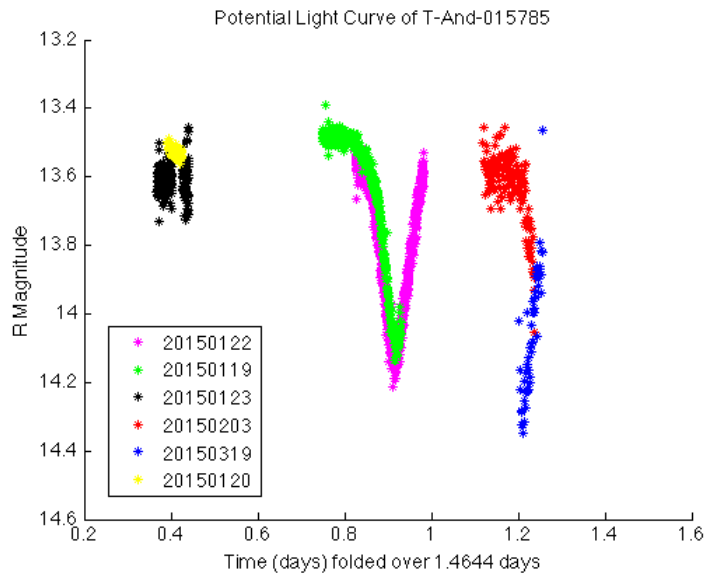


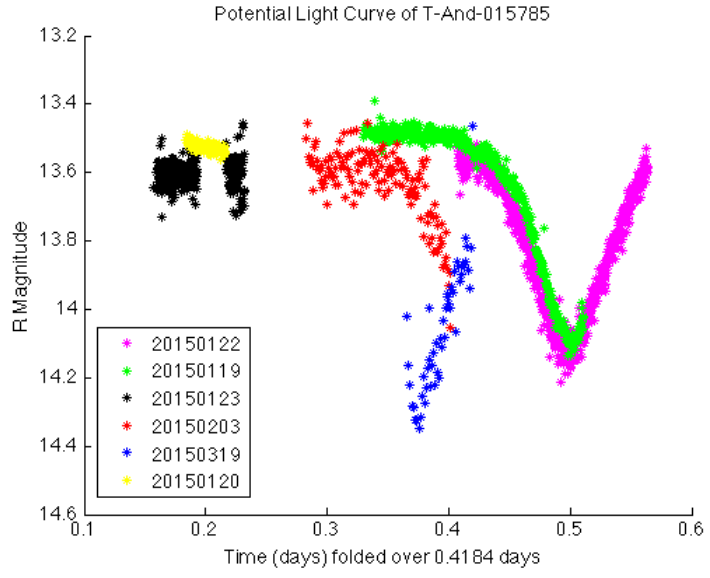
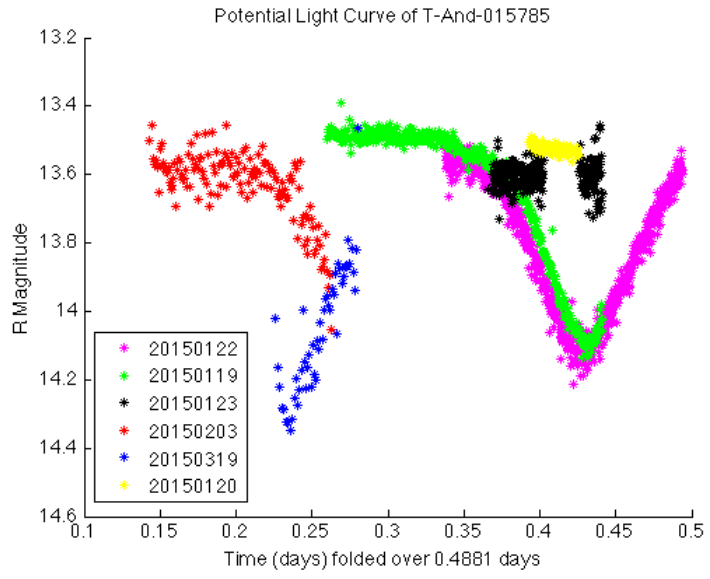
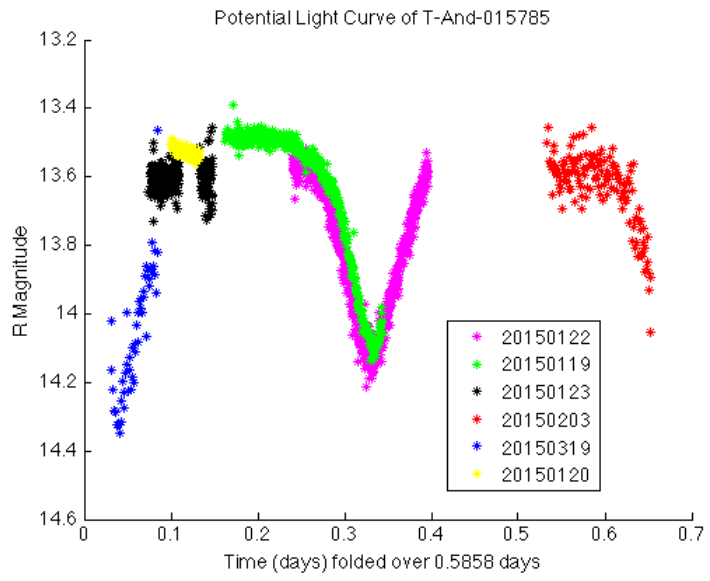
Figure 3-5: Folded T-And0-15785 Light Curve

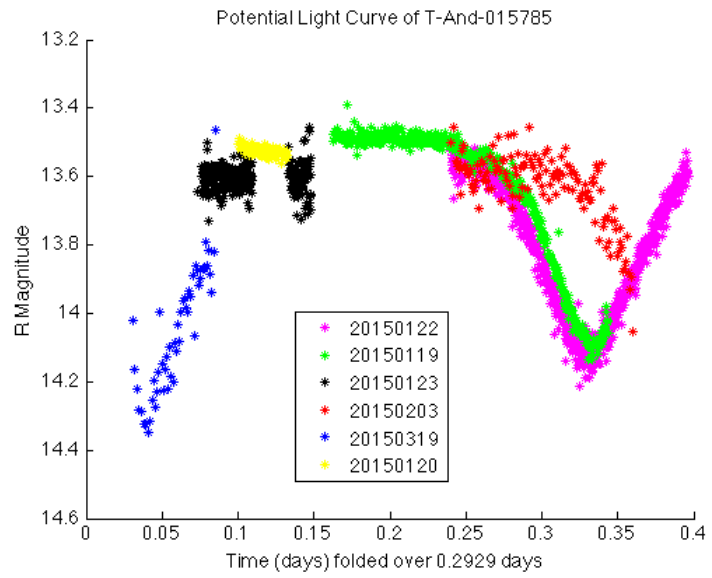
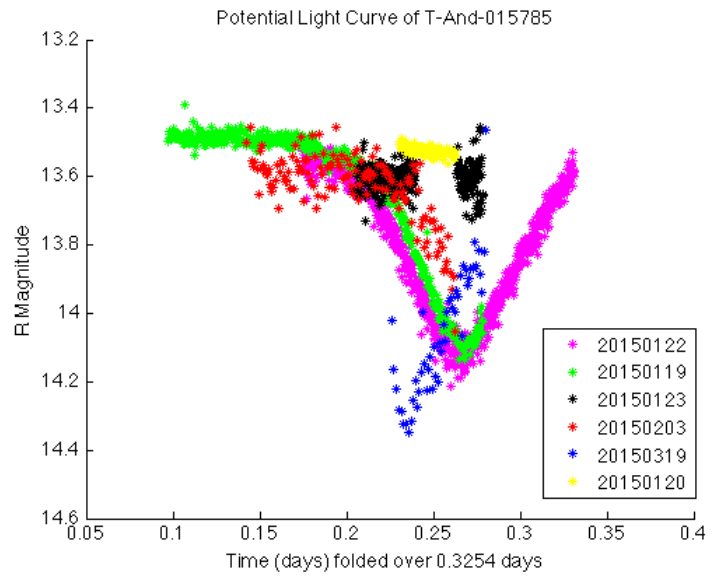
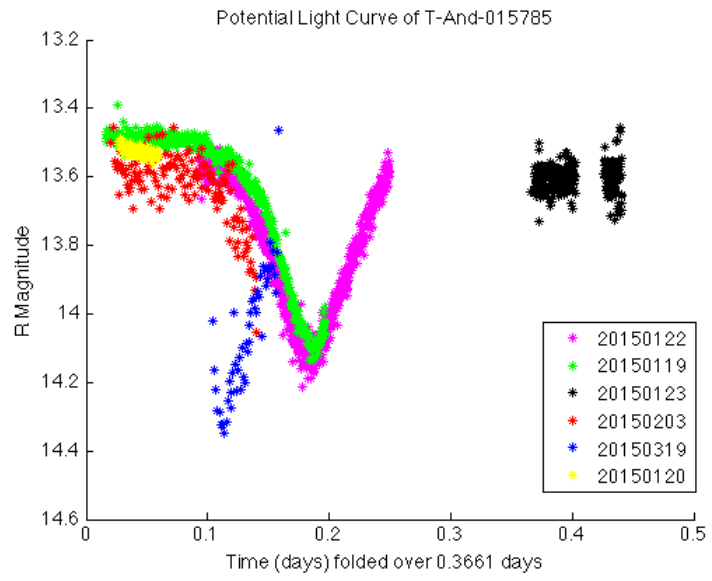
The Lorentzian fit was found for the primary eclipse by finding a Lorentzian fit of a compilation of the data for 3 February and 19 March. The eclipse was assumed to be symmetric and the complete fit was extrapolated from there. I concluded that the delta magnitude for the primary eclipse was 0.721 ± 0.0361 over a time period of 0.164 days. The Lorentzian fit was found for the secondary eclipse by finding a Lorentzian fit of a compilation of the data for 19 January and 22 January. I concluded that the delta magnitude for the secondary eclipse was 0.6196 ± 0.0309 over a time period of 0.212 days.

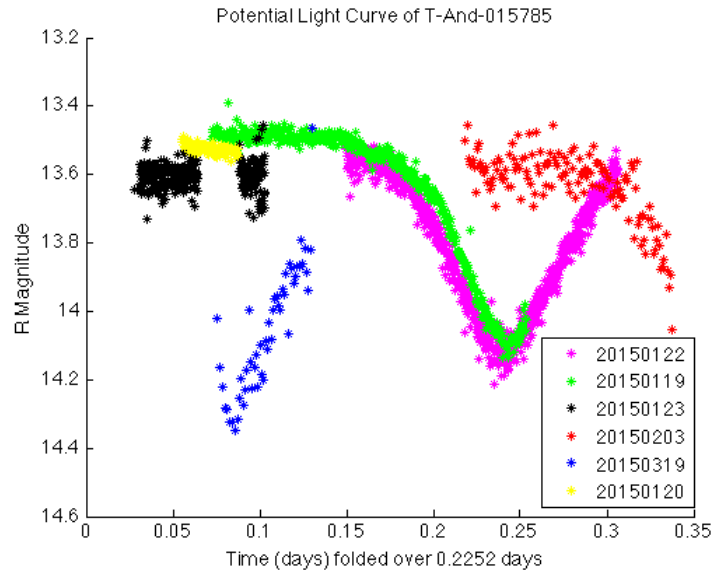
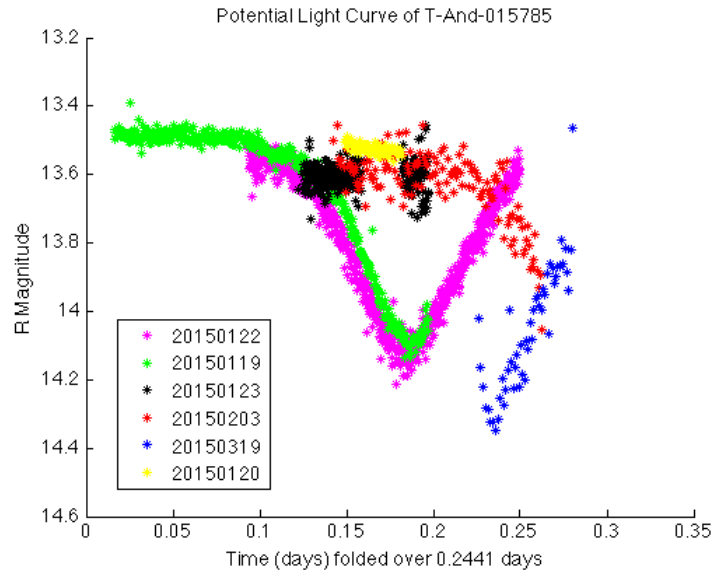
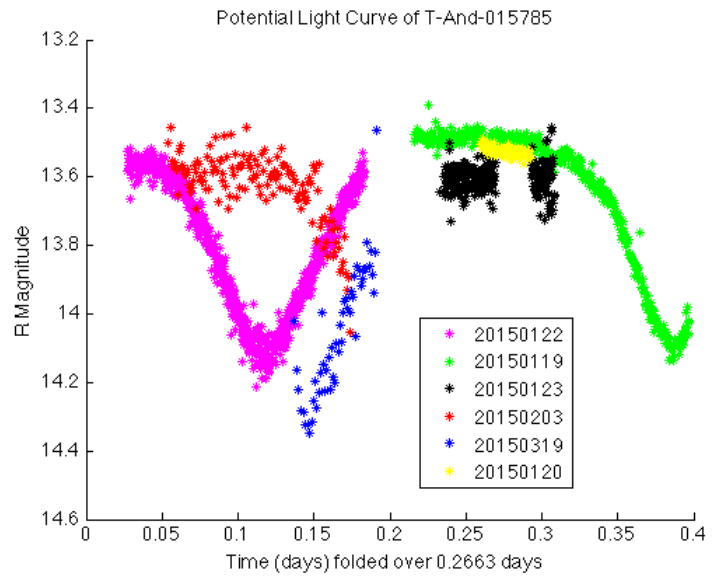
I also attempted to find the period of the eclipses from my data by assuming that the dip in magnitude found for 19 January and 22 January were both the same type of eclipse (ie. both primary or both secondary) since those two days were the only two that included the peak of the eclipse. I fit a Lorentzian to both of the nights and found the time difference between the peaks to be 2.9288 days. This time difference must be an integer multiple of the period of the eclipsing binary star. The period also must be longer than the time period covering one night of data (0.2035 days), considering that I did not view both eclipses. Therefore, the integer multiple must be between two and fourteen. I then graphed all of the data folded by $2.9288/n$ where $n = 2-14$; the graphs are shown in Figure 3.6.

Each graph shows what my data were to look like if the period of the eclipse was a different value. To find the value for the period of the eclipsing binary star, I examined the graphs for ones that did not have data points of various magnitudes overlapping temporally. It is necessary to take into account the time difference between the data taking sessions. A small error in the period will cause a large alteration when iterated over a lot of periods of the data. Considering this point, the data taken in March will be the least accurate since any small error in the period will have a large affect on where that data appears after folding according to the period. Therefore, when evaluating the accuracy of the period, more weight will be placed on the January and February data not conflicting than the data from March. Graphs with $n = 3$,









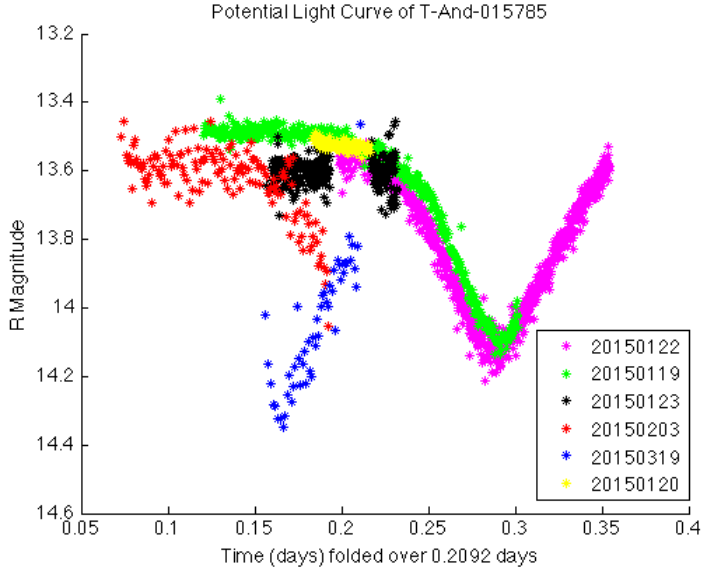


Figure 3-6: Period Testing of T-And0-15785. Each plot shows the T-And0-15785 light curve that my data create when folded over $2.9288/n$ where $n = 2-14$. If the curve has no conflicting data points, the value is a possible period for T-And0-15785.

6, 9, 12, and 14 have 23 January clearly conflicting with 19 January. Graphs with $n = 7, 9, 10, 11, 12, 13$ and 14 have 3 February clearly conflicting with 19 January. Graphs with $n = 4, 5$, and 8 do not clearly have any conflicting data, ignoring the March dataset; therefore, the period of 0.732 ± 0.0366 , 0.585 ± 0.0292 , or 0.366 ± 0.0183 days are the most likely.

The largest likely period, 0.732, and the smallest likely period, 0.366, differ by a factor of two. The two peaks of the binary star's light curve likely influenced these two periods. The smaller of the two periods would refer to the period between each peak, and the larger period refers to the period of the two peaks. Therefore, the most likely period of the binary star is 0.732. This value, 0.732 ± 0.0366 , is consistent with the literature value of 0.7311466 ± 0.0000095 [2].

3.4 Discussion

I calculated the baseline R-band magnitude for T-And0-15785 using data from 19 January and report the value as 13.487 ± 0.016 R magnitude. According to Devor, J. et. al 2008, T-And0-15785 has a baseline R magnitude of 13.380 [2]. These two values are within 0.1 magnitudes and therefore consistent.

T-And0-15785 has a primary and secondary eclipse. I have calculated the delta magnitude from the baseline R magnitude for the primary eclipse to be 0.721 ± 0.0361 R magnitudes and for the secondary eclipse to be 0.620 ± 0.0309 R magnitudes. These delta magnitudes are also consistent with Devor, J. et. al 2008, who says the delta magnitude for the primary eclipse is 0.703 R magnitudes and the delta magnitude for the secondary eclipse is 0.632.

I concluded that the period of T-And0-15785 is one of the following values: 0.732 ± 0.0366 , 0.585 ± 0.0292 , or 0.366 ± 0.0183 days. The most likely period of the three, 0.732 ± 0.0366 , is consistent with the period of 0.7311466 ± 0.0000095 [2].

Chapter 4

Conclusion

4.1 An Automated Dome and Telescope

I built and characterized the Small AUtonomous Robotic Optical Nightwatcher (SAURON) from 2014 through 2015 at the MIT George R. Wallace, Jr. Astrophysical Observatory. SAURON is a Schmidt-Cassegrain telescope housed in a ten-foot Technical Innovations ProDome. The telescope system currently functions as a robotic telescope, where data can be taken without physically accessing the telescope. This function allows students and faculty to use the telescope from campus instead of needing to drive out to the observatory.

The limiting magnitude of SAURON using the SBIG ST7-XME CCD is 17.3 R magnitudes. The full limiting magnitude calculation can be found in Appendix C. The readout speed is 2.4 seconds with 1x1 binning and no automatic reductions. The Root-mean-square (RMS) pointing is 14.5 arcsec. RMS pointing measures the statistical accuracy of the paramount as it points from one location in the sky to any other location in the sky. The population standard deviation (PSD) is 15.12 arcsec. The PSD shows the variance of the RMS over the entire sky. The maximum slew rate of the telescope is six degrees per second and the default slew rate is 5.4 degrees per second [9].

4.2 Future Work

SAURON has the potential to be fully autonomous. All of the components have been chosen with a goal of autonomy in mind. In order to make SAURON autonomous, three main upgrades need to be made to the telescope system. Firstly, the dome traction needs to be improved. Our plan is to remove the original traction material from the dome ring surface and coat this surface with paint that improves the traction. The new paint, along with continued improvement on the dome support wheels, should solve the dome traction issues. The second upgrade needed is the telescope and dome control software will need to move from The SkyX to a software that can take long term commands instead of immediate control commands. Our current software choice is CCDware autopilot. We plan on evaluating and testing CCDware autopilot Summer 2015 in order to autonomize SAURON. The final large upgrade is for our weather system. WAO currently has a weather system that reports the weather occurring at WAO so that observers can remotely operate the telescope from campus; however, this system cannot currently communicate with a telescope directly. We will need to upgrade the weather system's software so that it can send commands to SAURON so that SAURON can open in favorable weather and close before harmful weather arrives. After these improvements, WAO will have an autonomous telescope.

4.3 Long-Term Application

This autonomous telescope will increase the efficiency of data collection at WAO. It will encourage long-term projects to be pursued and save countless hours of observer time. For example, exoplanet candidates from the TESS mission can be monitored with small university observatory telescopes for multiple periods without requiring any observer time. This autonomous telescope ability to monitor a star without human interaction will save observers countless hours. After SAURON is a fully functioning autonomous telescope, WAO will begin to transform two more of the telescopes located at the observatory from robotic to autonomous. Assuming that the

autonomous telescopes located at WAO perform well, WAO can build an autonomous telescope in a remote location with optimal weather patterns in order to collect more data. Autonomous telescopes, in general, can improve many observatories used for teaching and research purposes and many undergraduate observing programs.

Appendix A

Component Specifications

Table A.1: OTA Specifications [1]

OTA	Celestron NexStar GPS
Aperature Diameter	11in (279mm)
Focal Length	110in (2800mm)
Focal Ratio	f10
Weight	65 lbs
Optical Design	Schmidt-Cassegrain
Limiting Magnitude	17.3

Table A.2: Mount Specifications [9]

Mount	SoftwareBisque Paramount ME II
Pointing Accuracy	30" or better (with Tpoint + supermodel)
Instrument Capacity	240 lbs
Maximum Payload	480 lbs
Counterweights used	60 lbs

Table A.3: PICO Detector Specifications [4]

Model	Finger Lakes Instrumentation ML261E-25
Read out rates	1.0 MHz or 2.8 MHz
Image Scale	1.4 arcsec/pixel
Field of View	12 arcmin x 12 arcmin
Exposure Times	0.1-3600s
Max Counts Unbinned	65,000
Pixel array	512 x 512
Pixel size	20 microns square

Table A.4: QSI Detector Specifications [10]

Model	QSI 683s CCD
Field of View	20 arcmin 57 arc sec x 15 arcmin 46 arcsec
Read out rates	Dual read rates of 800kHz and 8MHz
Image Scale	0.378 arcsec/pixel
Min/Max Exposure Times	0.12 - 3600s
Max Counts Unbinned	65,000
High Gain	0.5 e-/ADU (800KHz)
Low Gain	1.1 e-/ADU (8MHz)
Pixel array	3326 x 2504 pixels
Pixel Dimensions	5.4 microns square
Imager Size (WxH)	17.96mm x 13.52mm

Table A.5: SBIG Detector Specifications [8]

Model	SBIG ST7-XME
Field of View	8'2" x 5'21"
Read out time	2.4s
Image Scale	0.630 arcsec/pixel
Exposure Times	0.11 - 3600s
Max Counts Unbinned	40,000 high res, 65,000 low res
A/D Gain	2.6e-/ADU
Pixel array	765x510 pixels
Pixel Dimensions	6.9x4.6 mm
Pixel Size	9x9 microns square

Table A.6: Software

Program	Use
The SkyX Pro	Dome, Telescope, Camera control
Secure FX	Transferring data
MasterSync	Clock Syncing
DDW v5.4	Dome control
Chrome	Internet Access
AstroImageJ / MaximDL	Opening .fits files
TPoint	Correcting Mount Error
SBIG Driver 64	SBIG Camera Installation
Sophos endpoint security and control	Computer Security
Optec TCF-S 64	Focuser driver
FLI camera software + drivers	FLI Camera installation
Daily build v10.2	SkyX updates
CCDWare's CCDAutoPilot.	Automation

Appendix B

Photographs

B.1 Photographs of Build Process

B.2 Reference Photographs for Construction



(a) 24 June 2014 - Cutting the four foot concrete pier to six inches above the concrete pad.



(b) 3 July 2014 - The finished concrete pad with draining trench.



(c) 9 July 2014 - Leveling the mounting plate for the metal pier and paramount.



(d) 16 July 2014 - Unloading the dome with a forklift.



(e) 16 July 2014 - Laying out the dome on the concrete pad.



(f) 17 July 2014 - Leveling the metal pier.



(g) 22 July 2014 - Megan Russel, Rachel Aviles, and I constructing the dome ring.



(h) 22 July 2014 - Rachel Aviles and I circularizing the base rings.



(i) 22 July 2014 - Tim Brothers drilling into the concrete pad to attach the base ring.



(j) 22 July 2014 - Tim Brothers attaching the dome to the dome rings



(k) 22 July 2014 - Megan Russel attaching the shutter to the dome.



(l) 18 July 2014 - Olivia Brode-Roger milling shims to level the dome.



(m) 23 July 2014 - The completed dome.



(n) 13 Nov 2014 - Completed telescope setup inside of the dome.



(o) 29 Jan 2015 - Dome buried under three feet of snow.

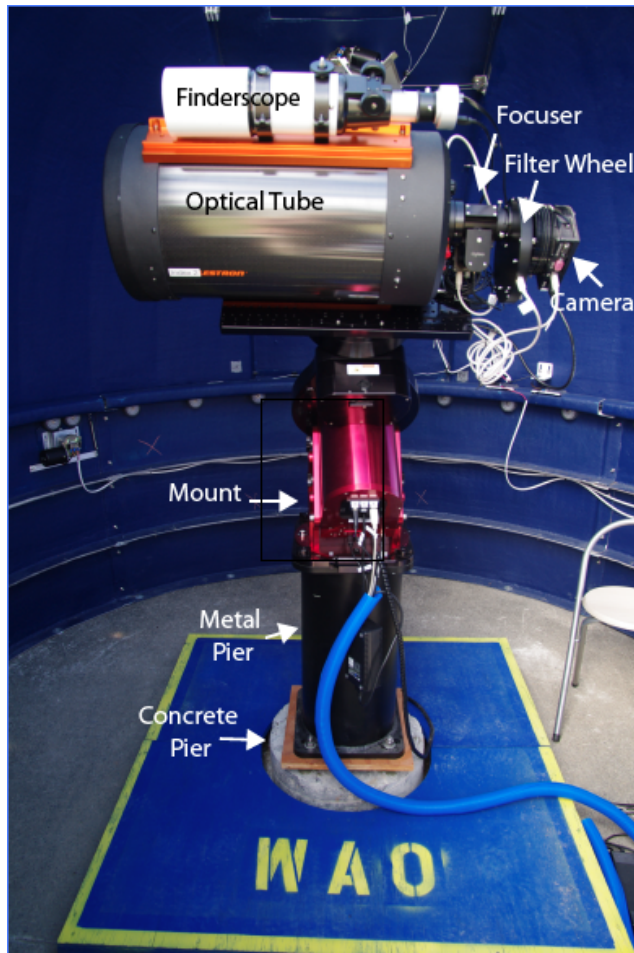
Figure B-1: Photos of Build Process



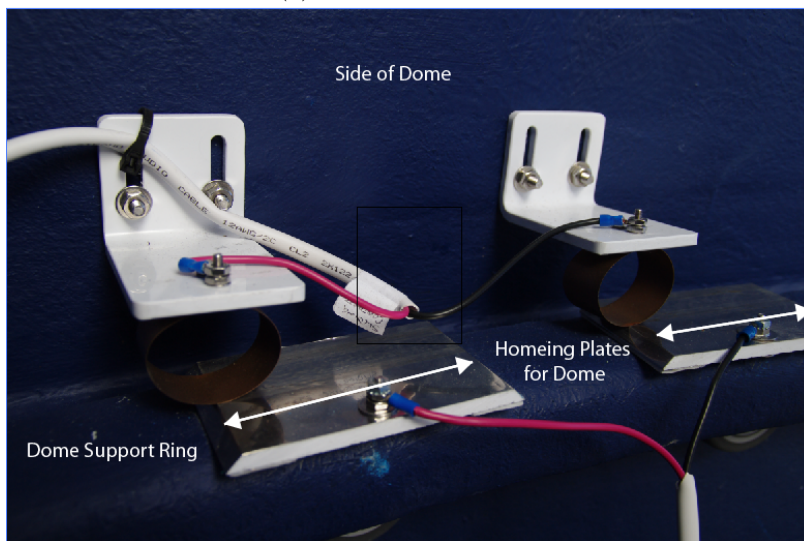
(a) Dome Frontview



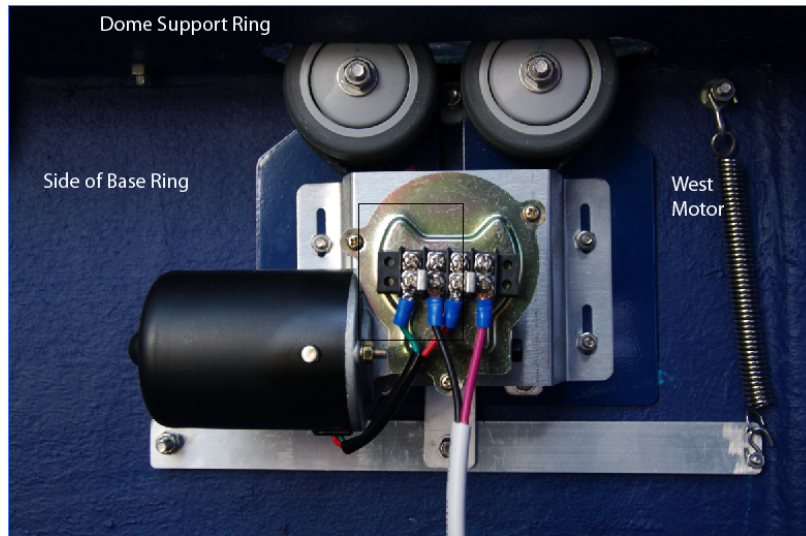
(b) Dome Sideview



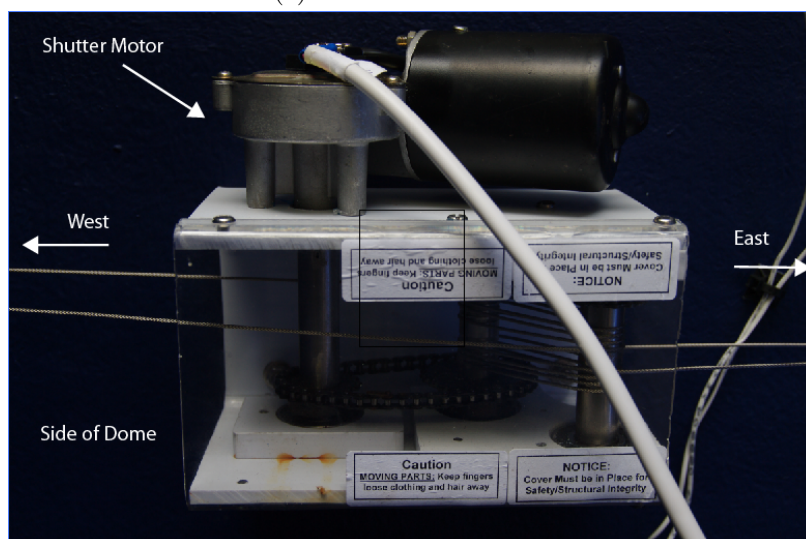
(c) Telescope System



(d) Dome Homing Plates



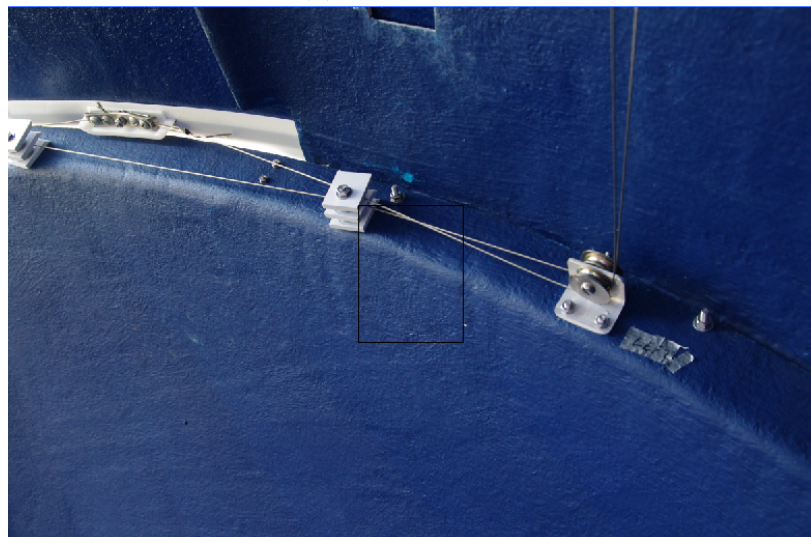
(e) Dome West Motor



(f) Shutter Motor



(g) Shutter Clamp



(h) Shutter Cables

Figure B-2: Dome Parts

Appendix C

Limiting Magnitude Calculation

To find the limiting magnitude of SAURON equipped with an SBIG ST7-XME camera, I took an image of the Pleiades and identified the stars within the field using the USNO A2.0 Catalogue [7] to find the magnitude of the faintest star in the image.

I first attempted to calculate the magnitude of the faintest star in the field by using the brightest ten stars in the field as comparison stars. Their R magnitudes were found in USNO catalogue [7]. Next, I used AstroImageJ to identify all other stars in the field. These target stars were referenced to the comparison stars with the same procedure as described in Chapter 3.3 in order to find their R magnitudes. The stars are shown in Figure C.1. The results of this analysis are shown in Table C.1.

The average difference between the calculated magnitude and the actual magnitude for all acceptable stars is 0.29 magnitudes different. I was unable to determine if all of the comparison stars were suitable since I did not have many images over time. Therefore, this analysis is inaccurate and cannot be reliably used. In order to find the limiting magnitude of the system, I used AstroImageJ to find all of the stars in this field, and searched the USNO A2.0 Catalogue [7] to determine the magnitudes of each star. The faintest star here has an R magnitude of 17.3. Since the Pleiades is an open cluster that contains stars of a wide range of magnitudes, the faintest star that can be identified can be assumed to be the limiting magnitude of the system.

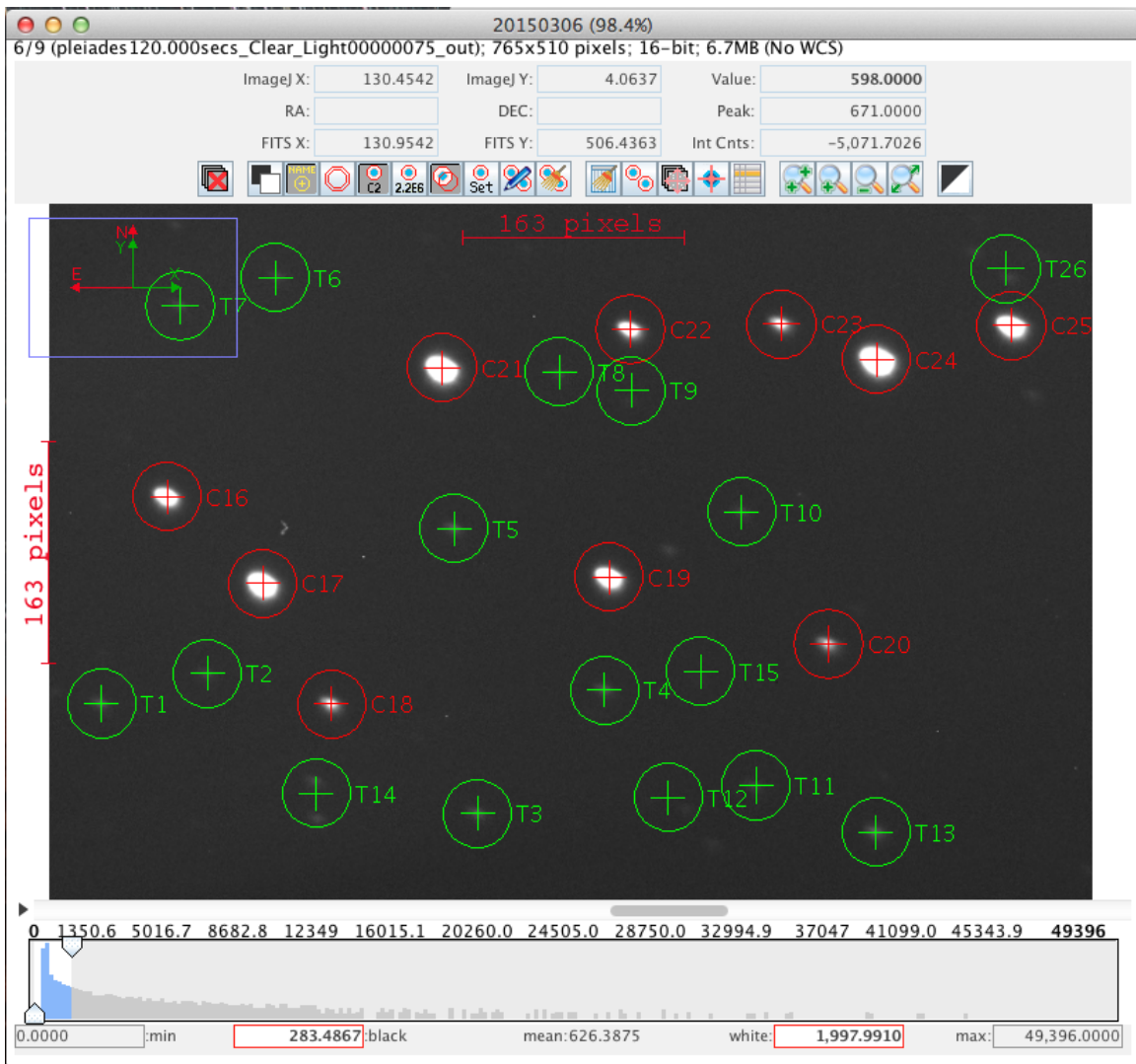


Figure C-1: Reduced Pleiades Image. All stars in the field were identified by AstroImageJ. The target stars are labeled 1-15, 26 and the comparison stars are labeled 16-25.

Table C.1: Limiting Magnitude Calculation

T#	Calculated Magnitude	Magnitude [7]	Difference	Acceptable?
T1	15.3	15.1	0.2	Yes
T2	16.0	15.6	0.4	Yes
T3	15.0	14.6	0.4	Yes
T4	15.1	14.9	0.2	Yes
T5	15.2	15.0	0.2	Yes
T6	16.0	15.9	0.1	Yes
T7	15.4	16.0	0.6	Yes
T8	16.5	15.5	0.2	No, star in background aperture
T9	12.2	16.2	4.0	No, aperture overlaps star
T10	16.0	15.7	0.3	Yes
T11	16.3	15.9	0.4	Yes
T12	16.8	16.6	0.2	No, centroid not found
T13	14.8	14.6	0.2	Yes
T14	14.8	15.3	0.5	No, multiple stars in aperture
T15	17.5	17.3	0.2	Yes
T26	15.7	16.3	0.6	No, aperture overlaps star

Bibliography

- [1] "CPC 1100 GPS (XLT) Computerized Telescope." Celestron. N.p., 2014. Web. 07 Apr. 2015.
- [2] Devor, Jonathan; Charbonneau, David; O'Donovan, Francis ; Mandushev, Georgi; Torres, Guillermo. "Identification, Classifications, and Absolute Properties of 773 Eclipsing Binaries Found in the Trans-Atlantic Exoplanet Survey." *The Astronomical Journal* 135.3 (2008): 850-77. Harvard ADS. Web. 17 Dec. 2014.
- [3] Dunham, E., M. Kosiarek, E. Markatou, and A. Wang. "Limits of Astrometric and Photometric Precision on KBOs." *PASP* 129.943 (2014): 863-67. Web.
- [4] Lockhart, Matthew, Michael J. Person, J. L. Elliot, and Steven P. Souza. "PICO: Portable Instrument for Capturing Occultations." *Publications of the Astronomical Society of the Pacific* 122.896 (2010): 1207-213.
- [5] MacRobert, Alan. "Accurate Polar Alignment." *Sky and Telescope*. N.p., 17 July 2006. Web. 07 Jan. 2015.
- [6] "MODEL ST-7XE/XME CCD IMAGING CAMERA." SBIG. Santa Barbara Instrument Group, 10 Feb. 2005. Web. 02 Apr. 2015.
- [7] Monet, et al. 1998, USNO-A2.0 Catalogue
- [8] "Operating Manual CCD Camera Models ST-7XE/XME, ST-8XE, ST-9XE, ST-10XE/XME and ST-2000XM/XCM With High Speed USB Interface." SBIG Astronomical Instruments. N.p., June 2004. Web. 02 Apr. 2015.

- [9] "Paramount ME II." Software Bisque. N.p., n.d. Web. 02 Apr. 2015.
- [10] "QSI 600 Series - Cooled CCD Cameras." QSI. Quantum Scientific Imaging, 2006-2013. Web. 10 Apr. 2015.
- [11] Ryden, Barbara Sue., and B. M. Peterson. Foundations of Astrophysics. San Francisco: Addison-Wesley, 2010. Print.
- [12] Shannon, Hall. "Life After Kepler: Upcoming Exoplanet Missions." Universe Today. N.p., 4 Nov. 2013. Web. 14 Jan. 2015.
- [13] Wells, Jered. "Lorentzian Fit." MATLAB Central. N.p., 15 Nov. 2011. Web. 03 Apr. 2015.